Response to reviewers' comments on Osadchiev et al., 'Influence of Estuarine Tidal Mixing on Structure and Spatial Scales of Large River Plumes' – original comments are in black, responses in blue.

Anonymous Referee #1

General comments

The manuscript describes using in-situ salinity observations to study the spatial scales and contrasting structures of two river plumes in the Arctic Ocean. The concept of freshwater volume is used to get new information from observational data and different vertical salinity structures in the two river plumes are demonstrated clearly. Even though one river has an order of magnitude greater discharge than the other, the limits of salinity concentrations consistent with spreading of riverine water are detected ~500km from both river mouths. Determining the processes that control riverine flow into the ocean is important for understanding the impacts of rivers on coastal and shelf regions. The manuscript is generally well written.

The title and abstract both mention tidal mixing as the primary process responsible for the observed differences in two river plumes. However, there is no analysis to demonstrate this in the manuscript. For the focus of the paper to be tidal mixing there needs to be some investigation of the processes involved. Another issue is that volumes and areas of the river plumes are inferred using data from one linear transect per river, but the justification for the calculations related to the width of the river plumes is not well argued (see specific comments).

Many thanks for your important comments that served to significantly improve the article. First, we added a new Section 3.1 focused on tidal circulation and tidal mixing in the Yenisei and Khatanga gulfs. Second, we added analysis of satellite observations of the Yenisei and Khatanga plumes, as well as extended the in situ data from two linear transects to support assessments of their spatial characteristics. We described and discussed new in situ and satellite data (Section 3.4), as well as analyzed wind forcing during the extended time periods (Section 3.2) that confirmed the assessments of spatial extents of the Yenisei and Khatanga plumes.

Specific comments

Line 20: The assertion that "rivers with similar discharge rates can form plumes with significantly different areas" is not supported by the data presented in the manuscript.

We agree that this statement is not supported by the data presented in the manuscript. This assertion was removed from the abstract.

Line 97: mean wind speed over 14 days of 7m/s is quite high and could include periods of strong wind speeds from different directions; plotting appropriate time series would give more information and show if wind forcing might impact on the river plume development.

According to your recommendation we added analysis of daily averaged wind speed and direction during 29 June – 26 July 2016 for the Yenisei plume and during 8 August – 18

September 2017 for the Khatanga plume. These wind time series cover ice-free periods at the study areas from decline of ice coverage to in situ measurements in the Yenisei and Khatanga plumes, i.e., the periods when wind forcing can influence river plumes. In Section 3.2 we provide analysis of these time series and showed that speed of the considered wind forcing was mainly moderate and low. In particular, the longest observed periods of continuous moderate and strong wind (> 5 m/s) were only 4 days in the central part of the Kara Sea and 3 days in the western part of the Laptev Sea. Wind direction during the study periods was highly variable due to high variability of atmospheric pressure accompanied by multiple cyclones and anticyclones. As a result, the wind forcing averaged during 2-week time periods is characterized by even more low wind speed (< 4 m/s) for the considered periods. Therefore, we presume that the Yenisei and Khatanga plumes were only weakly affected by wind forcing during the periods preceding the in situ measurements. As a result, the registered spatial extents of the Yenisei and Khatanga plumes depend mainly on river discharge conditions and estuarine mixing. This issue was clarified in the text.

Line 117 and figures 3b and 4b: the plotted freshwater fractions are not consistent with the definition given: eg S = 15 => F = (32 - 15) / 32 = 0.53 not 1 – 1.5% (which is plotted).

Many thanks for this comment. In this study we calculated the fraction $(S_0 – S) / S$, i.e., the ratio between volumes of river water V_{river} and sea water V_{sea} in the water parcel, not the fraction $(S_0 – S) / S_0$, i.e., the ratio between volume of river water V_{river} and total volume $V_{river} + V_{sea}$ of the water parcel, as it was incorrectly written in the text. This mistake was corrected in the text, and in the related figures.

Figures 3c and 4c: How was the "total share of FV among SL" derived?

In order to assess dilution of freshwater discharge within the Yenisei plume, we defined five different salinity ranges of river plume water, namely, $0 < S < 5$, $5 < S < 10$, $10 < S < 15$, $15 < S < 20$, $20 < S < 25$, as well as the salinity range $S > 25$ for the ambient sea. Then for all vertical salinity profiles of the transect we calculated local shares of freshwater volume in water column among these salinity ranges, i.e., what percentage of total freshwater volume contained in the water column is located between the isohalines of 0 and 5 (salinity range of 0-5), between the isohalines of 5 and 10 (salinity range of 5-10), etc. (Fig. 4c). Finally, we calculated total shares of freshwater volume in water column among these salinity ranges by averaging the reconstructed local shares of freshwater volume along the transect. This clarification was added to the text.

Line 128: the freshwater in different salinity layers is not a percentage volume since the changing width of the gulf is not accounted for.

In this part of the manuscript we describe the percentage of freshwater volume among different salinity ranges along the transect and do not state that it corresponds to the percentage volumes within the whole plumes. The related clarification was added to the text.

Lines 168-172: This section needs clarifying. In "This result is in good agreement with" etc: what result is being referred to? The data in the manuscript is for rivers with very different discharge rates not rivers with the same discharge rate. Is figure 6 and its description based on Fischer (1972) and Nash (2009)?

In this study we show that river discharge rate and estuarine tidal mixing are important factors that govern depth and area of a river plume. The Khatanga plume is an example of a river plume that experience strong tidal mixing in the estuary and occupies anomalously large area and volume (in relation to the river runoff rate) in the open sea. The Yenisei plume, on the opposite, experience low tidal mixing in the estuary, it is shallow and occupies relatively small area. Therefore, we demonstrate, that rivers with significantly different discharge rates (Yenisei and Khatanga) can form plumes with similar areas due to different intensity of estuarine mixing. This fact is supported by in situ measurements and satellite observations and is the main result of our work. This result is in a good agreement with Nash (2009) who showed that salinity and depth of a near-field plume are negatively correlated with a ratio of river discharge rate and cubed estuarine tidal velocity. We use freshwater fraction of a river plume, i.e., a ratio between volumes of river and sea water that were mixed to form a plume, as a proxy of its spatial extent, which is the main idea of the Figure 6. Therefore, we make an assumption that rivers with similar discharge rates can form river plumes with significantly different freshwater fractions and, therefore, spatial extents in case of large differences in intensity of estuarine mixing. However, the detailed analysis of this assumption is beyond the current study that was clearly stated in the text. We removed the related discussion and figure from the revised version of the manuscript.

Lines 186-194: The authors suggest that data from transects are representative of total surface areas of the river plumes because the Yenisei and Khatanga are 'large rivers' and so the plumes have similar zonal and meridional extents. However, the cited references [Pavlov et al., 1996; Zatsepin et al., 2010; Zavialov et al., 2015] show high variability in size and shape of the Yenisei and Khatanga river plumes. Also, it is possible in figure 5a) that some of the freshwater in the "Yenisei plume" comes from the nearby Ob River (Zavialov et al 2015; Osadchiev et al 2017).

We agree that the data from individual transects is not enough convincing for analysis of areas of the Yenisei and Khatanga plumes. Therefore, we processed and analyzed satellite observations of the Yenisei and Khatanga plumes to reconstruct their spreading areas. Also, based on satellite data, we distinguished the Ob and Yenisei plumes within the joint Ob-Yenisei plume in the central part of the Kara Sea. Based on joint analysis of satellite and in situ data, we detected spreading areas of the Yenisei and Khatanga plumes and show that, first, spatial extents of the Yenisei and Khatanga plumes were similar during the periods of field measurements, and, second, large spreading area of the Khatanga plume was regularly registered at cloud-free satellite imagery acquired in 2000-2019.

Lines 220-230: the calculation of the freshwater volume. Is this just for the limits of the two gulfs, or does it include the river plumes? Do the changing widths of the gulfs and plumes impact this calculation? What about flow to the ocean through other channels (both gulfs split in two at the seaward end)? In line 228, the agreement between the ratios of freshwater volume and river discharges isn't exactly "proof" that the transects can be used to infer freshwater volume.

We agree that calculation of these freshwater volume are not enough convincing due to changing widths of the gulfs, variability of salinity across the gulfs, and presence of shallow, but wide secondary channels that connect these gulfs with the sea. We omitted this paragraph from the revised version of the manuscript.

Web links to access the river discharge and atmospheric data used in the analysis are included but there is no information about access to the salinity observations.

According to your recommendation, we supplementary information with in situ data used in the study.

Technical corrections

Line 13: exhibits -> experiences.

Line 17: delete "obtained"

Line 47: accounts to -> accounts for.

Line 58: Kowalik and Proshutinsky, 1994 is missing from the references list.

Line 100: the date "24-18 September" is wrong in the caption. The colour palette is not very effective – could omit the range 1000-1010 hPa.

Lines 110 and 139: "several meters" lacks precision.

Line 121: insert "." after 2015]

Line 125: omit "far".

Figure 5: need to label that the discharge rates are shown, and check their units. Also specify which part of the water column.

Figure 6: freshwater fraction values should be less than 1.

Line 217 was spreading -> spread

Line 235: omit "getting".

Line 313: Kulikov et al. doi reference is incomplete.

Thank you for these minor comments, we made the related corrections in the text.

Anonymous Referee #2

The paper presents very interesting observations of two major river plumes in the Arctic basin. There is a paucity of such information in the oceanographic literature, so the paper certainly merits publication in the Ocean Science. However, some details of the data analysis and interpretation need improvements.

In my opinion, the authors pay too much attention to the fact that the outflows from the Yenisei Gulf and the Khatanga Gulf form plumes of roughly the same offshore extension, although the freshwater discharges of the two rivers differ by an order of magnitude (~30,000 mˆ3/s for the Yenisei River vs ~3,000 mˆ3/s for the Khatanga River). According to the authors, this happens due to the different intensity of tidal mixing in the two gulfs. I think this observation is rather trivial and obvious. Besides, it's not entirely accurate.

First, the Yenisei River plume indeed separates from the coast and extends offshore (northward) over 300 km from the estuarine mouth. The Khatanga River plume on the other hand remains attached to the Taymyr Peninsular coastline on its left flank (facing downstream) so its northward spreading cannot be characterized as the offshore extension (even more so in August 2000).

Thank you for this important comment. We agree that the data from individual transects is not enough convincing for analysis of areas of the Yenisei and Khatanga plumes. Therefore, we provided analysis of satellite observations of the Yenisei and Khatanga plumes in the revised version of the manuscript. Based on joint analysis of satellite and in situ data, we detected spreading areas of the Yenisei and Khatanga plumes and validated them against in situ measurements. We showed that, first, spatial extents of the Yenisei and Khatanga plumes were similar during the periods of field measurements, and, second, large spreading area of the Khatanga plume was regularly registered at cloud-free satellite imagery acquired in 2000-2019.

Second, the wind forcing, while weak, is upwelling-favorable for the Khatanga River plume (in 2017) and is downwelling-favorable for the Yenisei River plume. The authors do not describe the wind forcing conditions prior to shipboard surveys, and the plumes of such spatial scales can keep a "memory" of the wind forcing on time scales of a week or even more if the wind is not strong. So the wind field snapshots at the time of measurements are not entirely convincing.

According to your recommendation we added analysis of daily averaged wind speed and direction during 29 June – 26 July 2016 for the Yenisei plume and during 8 August – 18 September 2017 for the Khatanga plume. These wind time series cover ice-free periods at the study areas from decline of ice coverage to in situ measurements in the Yenisei and Khatanga plumes, i.e., the periods when wind forcing can influence river plumes. In Section 3.2 we provide analysis of these time series and showed that speed of the considered wind forcing was mainly moderate and low. In particular, the longest observed periods of continuous moderate and strong wind (> 5 m/s) were only 4 days in the central part of the Kara Sea and 3 days in the western part of the Laptev Sea. Wind direction during the study periods was highly variable due to high variability of atmospheric pressure accompanied by multiple cyclones and anticyclones. As a result, the wind forcing averaged during 2-week time periods is characterized by even more low wind speed (< 4 m/s) for the considered periods. Therefore, we presume that the Yenisei and Khatanga plumes were only weakly affected by wind forcing during the periods preceding the in situ measurements. As a result, the registered spatial extents of the Yenisei and Khatanga plumes

depend mainly on river discharge conditions and estuarine mixing. This issue was clarified in the text.

I also somewhat disagree with the authors' interpretation of the plume structure formed by large rivers (lines 187-190, page 11): In fact, both "medium-size" and "large" (author's terminology) river plumes have the anticyclonic bulge region near the mouth and the semi-geostrophic, narrower coastal current farther downstream, as long as the Coriolis force is important. In this regard, the Amazon River and the Congo River plumes are not quite relevant since they are near the equator, while other major river plumes do have both a bulge region and a coastal current (far field), including the Mississippi plume, The Yangtze plume, the La Plata plume, the Columbia River, the Danube River, the Siberian rivers, etc.

We totally agree that large river plumes have asymmetric shapes that result in their different cross-shore and alongshore extents. However, in this part of the manuscript we expressed the idea that cross-shore extents of large river plumes near their estuaries are more stable that those of small river plumes. Anyway, in the revised version of the manuscript we omitted this statement and the related discussion because we quantified the similarity of areas of the Yenisei and Khatanga plumes based on satellite observations described in Section 3.4.

Some minor issues with the manuscript:

Line 46 and later: I think it's better to use mˆ3 /s units for the freshwater discharge throughout the text.

Line 58: ": : :tidal amplitude and velocity: : :" Amplitude of what, perhaps the free surface? As for the velocity, is it also an amplitude or rms?

Line 86: ": : :performed at 100 m spatial resolution: : :". How can it be? I thought the water was pumped continuously under way. Do the authors imply the averaging interval here?

Line 92: ": : :and 200 km far from the river mouths: : :". "Far" is not needed here.

Line 107:" : : :Kara Sea shelf (stations 5336-5350)." The statement is misleading; it should read "stations 5333-5336 and 5349-5350".

Lines 123-124: "As a result, the majority of river runoff propagated off the estuary: : :". This is a somewhat strange proposition; the riverine discharge should "propagate off the estuary", otherwise there will a freshwater flux convergence in the estuary and the estuary will be continuously getting fresher.

Line 126 and below: ": : :was located in two salinity layers: : :". "Layer" is not a good choice in this context; it is one buoyant layer, just comprising different salinity classes or ranges or whatever word the authors would prefer.

Line 138: Is the salinity gradient in this context "stable" or constant?

Thank you for these minor comments, we made the related corrections in the text.

Influence of Estuarine Tidal Mixing on Structure and Spatial Scales of Large River Plumes

Alexander Osadchiev[1,2], Igor Medvedev[1,3], Sergey Shchuka[1], Mikhail Kulikov[1], Eduard Spivak[3~~4~~], Maria Pisareva[1], Igor Semiletov[3~~4~~]

[1]Shirshov Institute of Oceanology, Russian Academy of Sciences, Moscow, Russia
[2]Institute of Geology of Ore Deposits, Petrography, Mineralogy and Geochemistry, Russian Academy of Sciences, Moscow, Russia
[3]Fedorov Institute of Applied Geophysics, Roshydromet, Moscow, Russia
[3~~Ilyichov~~ 4]Ilyichov Pacific Oceanological Institute, Far Eastern Branch of the Russian Academy of Sciences, Vladivostok, Russia

Correspondence to: Alexander Osadchiev (osadchiev@ocean.ru)

Abstract. The Yenisei and Khatanga rivers are among the largest estuarine rivers that inflow to the Arctic Ocean. Discharge of the Yenisei River is one order of magnitude larger than that of the Khatanga River. However, spatial scales of buoyant plumes formed by freshwater runoffs from the Yenisei and Khatanga gulfs are similar. This feature is caused by different tidal forcing in these estuaries, which have similar sizes, climate conditions, and geomorphology. The Khatanga discharge ~~exhibits~~ experiences strong tidal forcing that causes formation of a diluted bottom-advected plume in the Khatanga Gulf. This anomalously deep and weakly-stratified plume has a small freshwater fraction and, therefore, occupies a large area on the shelf. The Yenisei Gulf, on the other hand, is a salt-wedge estuary that receives a large freshwater discharge and is less affected by tidal mixing due to low tidal velocities. As a result, the low-salinity and strongly-stratified Yenisei plume has a large freshwater fraction and its horizontal size is relatively small. The ~~obtained~~ results show that estuarine tidal mixing determines freshwater fraction in these river plumes, which governs their depth and area after they spread from estuaries to coastal sea. Therefore, influence of estuarine mixing on spatial scales of a large river plume can be of the same importance as the roles of river discharge rate and wind forcing. In particular, ~~rivers with similar discharge rates can form plumes with significantly different areas, while~~ plumes with similar areas can be formed by rivers with significantly different discharge rates that is illustrated by the Yenisei and Khatanga plumes.

1 Introduction

River plumes play an important role in land-ocean interactions. Despite their relatively small volume as compared to adjacent coastal seas, they significantly affect global fluxes of buoyancy, heat, terrigenous sediments, nutrients, and anthropogenic pollutants, which are discharged to the coastal ocean with continental runoff [Dagg et al., 2004; Milliman and Farnsworth, 2011; Lebreton et al., 2017; Schmidt et al., 2017]. As a result, dynamics and variability of river plumes are key factors for understanding mechanisms of spreading, transformation, and redistribution of continental discharge and river-

borne constituents in coastal seas and their influence on adjacent continental shelves [Geyer et al., 2004; Hickey et al., 2010; Hetland and Hsu, 2013]. World river plumes are characterized by wide variety of structure, morphology, and dynamical characteristics caused by large differences in regional features [Chant, 2011; Horner-Devine et al., 2015; Osadchiev and Korshenko, 2017; Osadchiev and Sedakov, 2019; Zavialov et al., 2020], in particular, estuarine conditions [Guo and Valle-Levison, 2007; Nash et al., 2009; Lai et al., 2016; Osadchiev, 2017].

River estuaries are areas where freshwater discharge initially interacts with saline sea water. The related processes of mixing of river runoff with sea water and formation of river plumes in estuaries determine their structure and govern their subsequent spreading and mixing in open sea. Intensity of estuarine mixing varies from negligible, when mostly undiluted freshwater discharge inflows directly to coastal sea, to dominant, which results in significant dilution of river discharge in well-mixed enclosed basins before being released to open sea [Schettini et al., 1998; Halverson and Palowicz, 2008; MacCready and Geyer, 2010; Geyer and MacCready, 2014].

The Yenisei and Khatanga estuaries are among the largest that flow into the Arctic Ocean (Fig. 1). These Yenisei and Khatanga gulfs are closely located and have similar sizes, geomorphology, and climatic conditions, albeit significantly different tidal forcing. In this study we focus on transformation of discharge of the Yenisei and Khatanga rivers in their estuaries and spreading of their buoyant plumes that occupy wide areas in the Kara and Laptev seas. Discharge of the Yenisei River is one order of magnitude larger than of the Khatanga River. However, spatial scales of buoyant plumes formed by freshwater runoffs from the Yenisei and Khatanga gulfs are similar. Using in situ hydrographic data, we reveal that this feature is caused by difference in intensity of estuarine tidal mixing that greatly affects spatial scales of these river plumes.

The paper is organized as follows. Section 2 provides the detailed information about the study area, the in situ, satellite, and wind reanalysis data used in this study. Section 3 describes the vertical structures and spatial extents of the Yenisei and Khatanga plumes, as well as tidal and wind forcing conditions in the study area. The influence of estuarine tidal forcing on spreading and mixing of the Yenisei and Khatanga plumes is analysed in Section 4 followed by the conclusions in Section 5.

2 Study area and data

2.1 Study area

Freshwater discharge from the Yenisei River (630 km^3 annually or 20000 m^3/s on average) is the largest among the Arctic rivers and accounts for 20% of total freshwater runoff to the Arctic Ocean [Gordeev et al., 1996; Carmack, 2000]. Hydrological regime of the Yenisei River is governed by a distinct freshet peak in June – July (half of total annual discharge), moderate discharge in May and August – September, and a drought in October – April [Pavlov et al., 1996; Guay et al., 2001]. The Yenisei River inflows into the Yenisei Gulf located at the southeastern part of the Kara Sea at the western side of the Taymyr Peninsula (Fig. 1a). The Yenisei Gulf is 250 km long; its width is 35-50 km. Average depth of the

southern (inner) part of the gulf increases off the river mouth from 5 to 15 m. The large Sibiryakov Island is located in northern (outer) part of the gulf and divides it into two 40-50 km long and 30-35 km wide straits (Fig. 1b). The western strait between the Sibiryakov and Oleniy islands is shallow (10 m deep), while depth of the eastern strait between the Sibiryakov Island and the Taymyr Peninsula steadily increases towards the open sea to 25-30 m and connects the Yenisei Gulf with the central part of the Kara Sea. The Yenisei Gulf is covered by ice in October – July. Tides are relatively low in the Yenisei Gulf, maximal tidal range and velocity do not exceed 0.5 m and 0.3 m/s [Voinov, 2002].

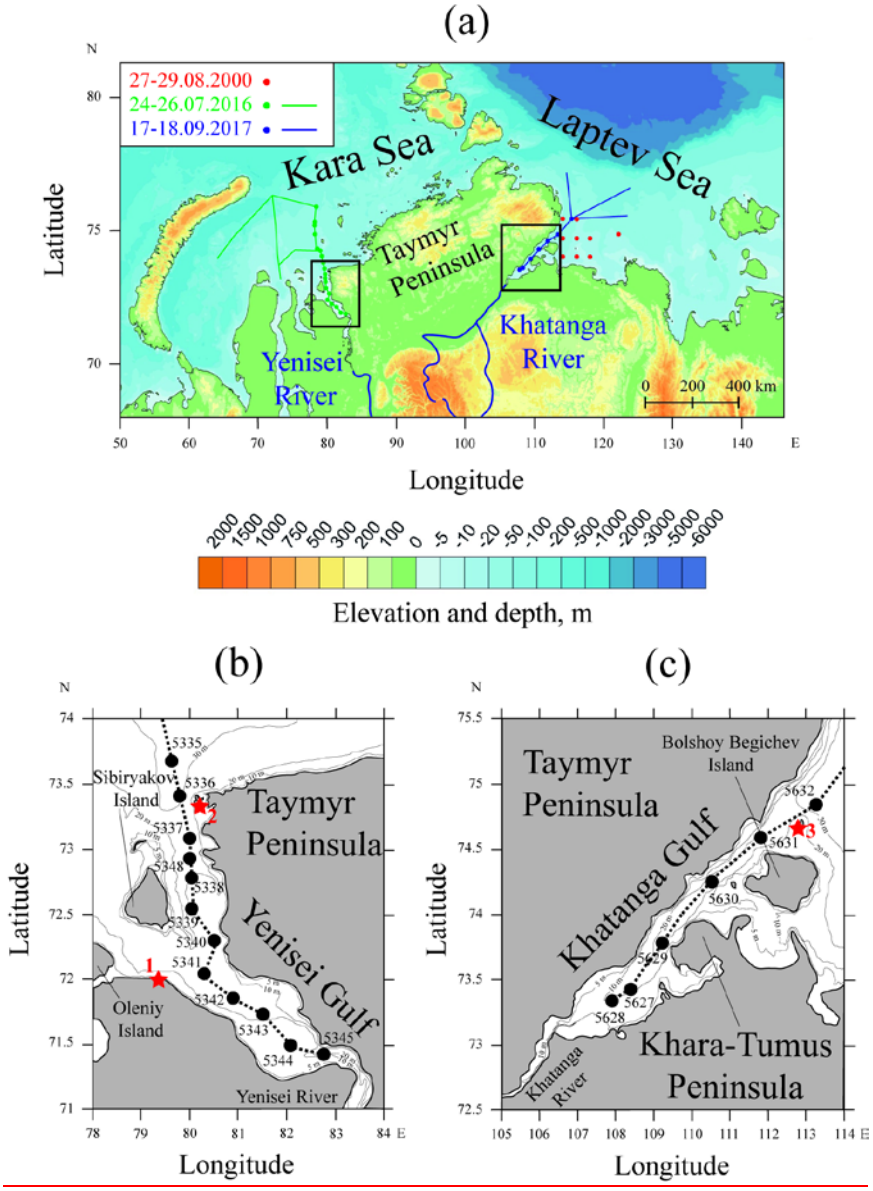

Figure 1: Study area; ship tracks (lines) and location of hydrological stations (circles) of three oceanographic field surveys conducted in August 2000 (red) and September 2017 (blue) in the Laptev Sea and in July 2016 (green) in the Kara Sea (a).

Bathymetry, ship tracks, and location of hydrological stations (black circles) and tidal gauge stations (red stars: 1 – Leskin, 2 – Dikson, 3 – Preobrazheniye) in the Yenisei (b) and Khatanga (c) gulfs. Black boxes in panel (a) indicate locations of the study areas in the Yenisei and Khatanga gulfs shown in panels (b) and (c). The graphic scale in panel (a) corresponds to the latitude of 73°.

Freshwater discharge from the Khatanga River (105 km^3 annually or 3300 m^3/s on average) is much smaller than that from the Yenisei River. Approximately one half of this volume is discharged to the Laptev Sea during a freshet period in June and then the river discharge steadily decreases till September [Pavlov et al., 1996]. The lower part of the Khatanga River is completely frozen in October – May and river discharge is negligible during this period [Pavlov et al., 1996]. The Khatanga River inflows into the Khatanga Gulf which is located at the southwestern part of the Laptev Sea at the eastern side of the Taymyr Peninsula (Fig. 1a). Shape, bathymetry, spatial scales, and climatic conditions of the Khatanga Gulf are similar to those of the Yenisei Gulf which is located approximately 800 km to the west from the Khatanga Gulf. The Khatanga Gulf is 250 km long; its width is 25-50 km. The shallow (5-20 m deep) inner and deep (20-30 m deep) outer parts of the gulf are connected by a narrow strait (15-20 km wide) between the Khara-Tumus and Taymyr peninsulas (Fig. 1c). The Bolshoy Begichev Island is located in the outer part of the Khatanga Gulf and divides it into two straits. The southern strait is narrow (8 km wide) and shallow (10 m deep), while depth of the northern strait (15-20 km wide) between the Bolshoy Begichev Island and the Taymyr Peninsula steadily increases towards the open sea to 25-30 m and connects the Khatanga Gulf with the western part of the Laptev Sea. The Khatanga Gulf is covered by ice in October – July. Tides in the Khatanga Gulf are among the largest in the Eurasian part of the Arctic Ocean. Maximal spring tidal range in different part of the gulf is 1-2 m [Korovkin and Antonov, 1938; Pavlov et al., 1996; Kulikov et al., 2018]. The largest tidal velocities up to 1.4-1.7 m/s were registered at the straits that connect the outer part of the gulf with the inner part and the open sea, which are described above [Korovkin and Antonov, 1938; Pavlov et al., 1996].

2.2 Data

Hydrographic in situ data used in this study were collected during three oceanographic field surveys in the Kara and Laptev seas including the 4th cruise of the R/V "Nikolay Kolomeytsev" on 27-29 August 2000 in the southwestern part of the Laptev Sea, the 66th cruise of the R/V "Akademik Mstislav Keldysh" on 24-26 July 2016 in the Yenisei Gulf and the central part of the Kara Sea, the 69th cruise of the R/V "Akademik Mstislav Keldysh" on 17-18 September 2017 in the Khatanga Gulf and the southwestern part of the Laptev Sea (Fig. 1). Field surveys included continuous measurements of salinity in the surface sea layer (2-3 m depth) performed along the ship track using a ship board pump-through system equipped by a thermosalinograph (*Sea-Bird Electronics SBE 21 SeaCAT*).. Vertical profiles of salinity were performed using a conductiveit-temperature-depth (CTD) instrument (*Sea-Bird Electronics SBE 911plus*) at 0.2 m vertical resolution. This CTD profiler was equipped with two parallel temperature and conductivity sensors; the mean temperature differences between them did not exceed 0.01°C, while differences of salinity were not greater than 0.01.

The tidal data used in this study includes in situ data from tidal gauge stations and results of tidal numerical modelling. We used hourly sea level records from two tide gauges located in the Yenisei Gulf, namely, Leskin and Dikson (indicated by red

stars in Fig. 1b and numbers 1 and 2, respectively), and the Preobrazheniye tide gauge station in the Khatanga Gulf (indicated by the red star and number 3 in Fig. 1c). Tidal gauge data were downloaded from the Unified State System of Information about the World Ocean (ESIMO) website (http://portal.esimo.ru/portal). Tidal velocity data in the study area were obtained from the Arctic Ocean Tidal Inverse Model (AOTIM5), version 2018 [Padman and Erofeeva, 2004]. The AOTIM5 is based on the data assimilation scheme [Egbert et al., 1994] and presents an inverse solution assimilating almost all available tide gauge data in the Arctic Ocean [Padman and Erofeeva, 2004]. The assimilated data consist of coastal and benthic tide gauges (between 250 and 310 gauges per constituent), 364 cycles of TOPEX/Poseidon and 108 cycles of ERS altimeter data. The model bathymetry is based on the International Bathymetric Chart of the Arctic Ocean (IBCAO) [Jakobsson et al., 2000] reprojected on a uniform 5-km grid. Tidal simulations were run in absence of sea ice.

Wind forcing conditions were examined using ERA5 atmospheric reanalysis with a 0.25° spatial and hourly temporal resolution. The reanalysis data were downloaded from the European Centre for Medium-Range Weather Forecasts (ECMWF) website (https://www.ecmwf.int/en/forecasts/datasets/archive-datasets/reanalysis-datasets/era5). Discharge data used in this study was obtained at the most downstream gauge stations at the Yenisei and Khatanga rivers located approximately 650 and 200 km far from the river mouths, respectively. The river discharge data were downloaded from the Federal Service for Hydrometeorology and Environmental Monitoring of Russia (FSHEMR) website (http://gis.vodinfo.ru/).

Satellite data used in this study include Terra/Aqua Moderate Resolution Imaging Spectroradiometer (MODIS) satellite imagery provided by the National Aeronautics and Space Administration (NASA). MODIS L1b calibrated radiances including MODIS bands 1 (red), 3 (blue), 4 (green), and daytime 31 (thermal) were downloaded from the NASA web repository (https://ladsweb.modaps.eosdis.nasa.gov/). We used ESA BEAM software for retrieving maps of sea surface distributions of corrected reflectance (CR), concentration of chlorophyll-a (Chl-a), and brightness temperature (BT) at the study areas with spatial resolutions of 500 m, 500 m, and 1 km, respectively. Chl-a distributions were calculated using the Ocean Color 3M (OC3M) algorithm [O'Reilly et al., 1998; Werdell and Bailey, 2005]. Due to the complexity of coastal processes that govern the temperature of the sea surface and the absence of specific regional algorithms for retrieving sea surface temperature (SST) from satellite data in the study areas with very limited in situ measurements, we did not used the standard SST product of MODIS. Instead, we used a BT product that does not provide an accurate temperature of the sea surface, but shows relative temperature differences, which can be used to detect spreading areas of the river plumes.

~~1 Introduction~~

~~River plumes play an important role in land-ocean interactions. Despite their relatively small volume as compared to adjacent coastal seas, they significantly affect global fluxes of buoyancy, heat, terrigenous sediments, nutrients, and anthropogenic pollutants, which are discharged to the coastal ocean with continental runoff [Dagg et al., 2004; Milliman and Farnsworth, 2011; Lebreton et al., 2017; Schmidt et al., 2017]. As a result, dynamics and variability of river plumes are key factors for understanding mechanisms of spreading, transformation, and redistribution of continental discharge and river-~~

borne constituents in coastal seas and their influence on adjacent continental shelves [Geyer et al., 2004; Hickey et al., 2010; Hetland and Hsu, 2013]. World river plumes are characterized by wide variety of structure, morphology, and dynamical characteristics caused by large differences in regional features [Chant, 2011; Horner-Devine et al., 2015; Osadchiev and Korshenko, 2017], in particular, estuarine conditions [Guo and Valle-Levison, 2007; Nash et al., 2009; Lai et al., 2016].

River estuaries are areas where freshwater discharge initially interacts with saline sea water. The related processes of mixing of river runoff with sea water and formation of river plumes in estuaries determine their structure and govern their subsequent spreading and mixing in open sea. Intensity of estuarine mixing varies from negligible, when mostly undiluted freshwater discharge inflows directly to coastal sea, to dominant, which results in significant dilution of river discharge in well-mixed enclosed basins before being released to open sea [Schettini et al., 1998; Halverson and Palowicz, 2008; MacCready and Geyer, 2010; Geyer and MacCready, 2014].

The Yenisei and Khatanga estuaries are among the largest that flow into the Arctic Ocean. These Yenisei and Khatanga gulfs are closely located and have similar sizes, geomorphology, and climatic conditions, albeit significantly different tidal forcing. In this study we focus on transformation of discharge of the Yenisei and Khatanga rivers in their estuaries and spreading of their buoyant plumes that occupy wide areas in the Kara and Laptev seas. Discharge of the Yenisei River is one order of magnitude larger than of the Khatanga River. However, spatial scales of buoyant plumes formed by freshwater runoffs from the Yenisei and Khatanga gulfs are similar. Using in situ hydrographic data, we reveal that this feature is caused by difference in intensity of estuarine tidal mixing that greatly affects spatial scales of these river plumes.

2 Study area

Freshwater discharge of the Yenisei River (630 km^3 annually) is the largest among Arctic rivers and accounts to 20% of total freshwater runoff to the Arctic Ocean [Gordeev et al., 1996; Carmack, 2000]. Hydrological regime of the Yenisei River is governed by a distinct freshet peak in June – July (half of total annual discharge), moderate discharge in May and August – September, and a drought in October – April [Pavlov et al., 1996; Guay et al., 2001]. The Yenisei River inflows into the Yenisei Gulf located at the southeastern part of the Kara Sea at the western side of the Taymyr Peninsula (Fig. 1). The Yenisei Gulf is 250 km long; its width is 35-50 km. Average depth of the southern (inner) part of the gulf increases off the river mouth from 5 to 15 m. The large Sibiryakov Island is located in northern (outer) part of the gulf and divides it into two 40-50 km long and 30-35 km wide straits (Fig. 1b). The western strait between the Sibiryakov and Oleniy islands is shallow (10 m deep), while depth of the eastern strait between the Sibiryakov Island and the Taymyr Peninsula steadily increases towards the open sea to 25-30 m and connects the Yenisei Gulf with the central part of the Kara Sea. The Yenisei Gulf is covered by ice in October – July. Tides are relatively low in the Yenisei Gulf, tidal amplitude and velocity do not exceed 0.5 m and 0.2 m/s [Kowalik and Proshutinsky, 1994; Padman and Erofeeva, 2004; Kagan et al., 2010, 2011].

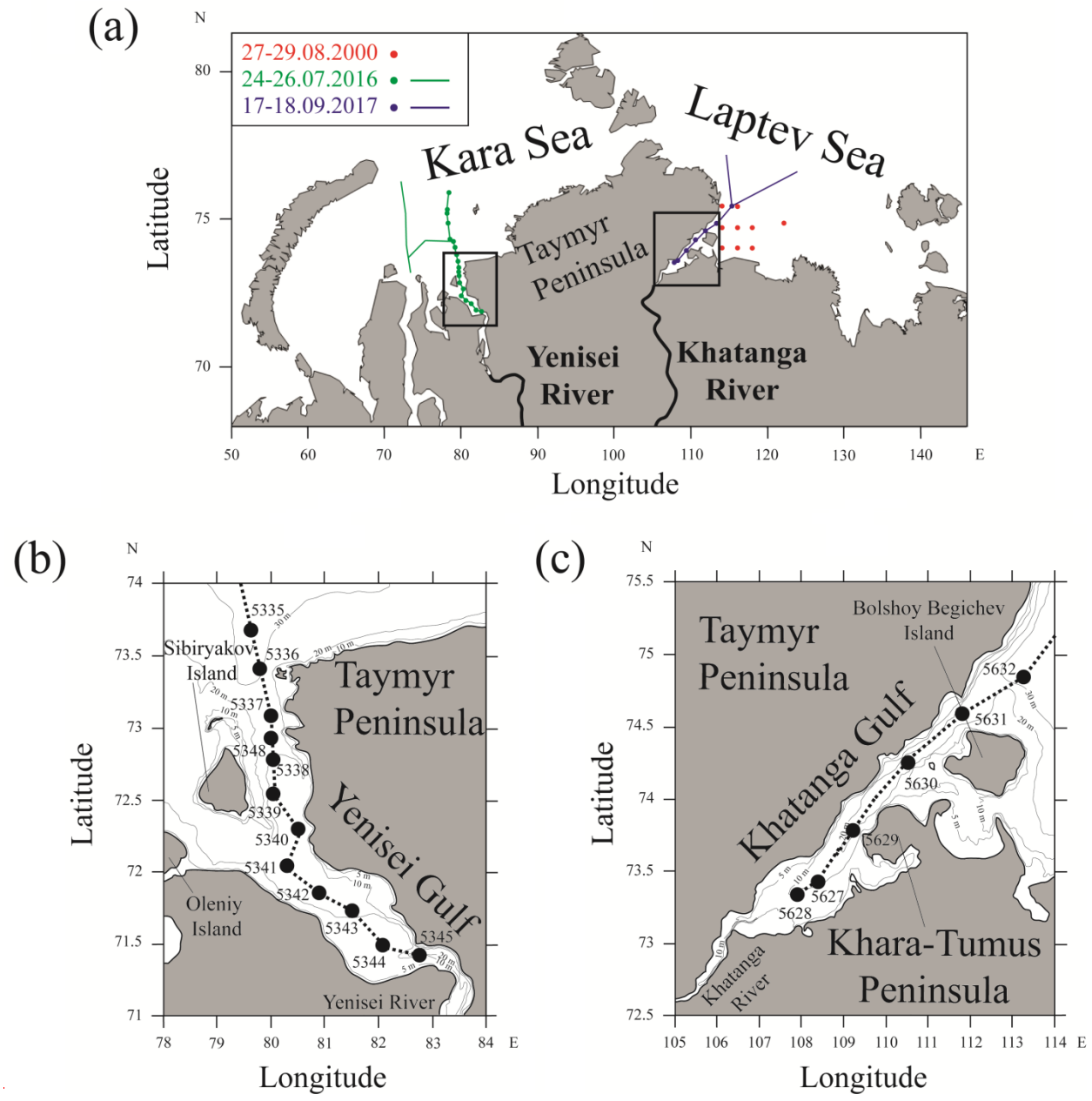

~~Figure 1: Study area; location of the Yenisei and Khatanga gulfs; ship tracks (lines) and location of hydrological stations (circles) of three oceanographic field surveys conducted in August 2000 (red) and September 2017 (blue) in the Laptev Sea and in July 2016 (green) in the Kara Sea (a). Bathymetry, ship tracks, and location of hydrological stations in the Yenisei (b) and Khatanga (c) gulfs.~~

~~Freshwater discharge of the Khatanga River (105 km^3 annually) is much smaller than that of the Yenisei River. Approximately one half of this volume is discharged to the Laptev Sea during freshet period in June, then the river discharge steadily decreases till September [Pavlov et al., 1996]. The lower part of the Khatanga River is completely frozen in October~~

~~– May and during this period its discharge is negligible [Pavlov et al., 1996]. The Khatanga River inflows into the Khatanga Gulf which is located at the southwestern part of the Laptev Sea at the eastern side of the Taymyr Peninsula (Fig. 1). Shape, bathymetry, spatial scales, and climatic conditions of the Khatanga Gulf are similar to those of the Yenisei Gulf which is located approximately 800 km to the west from the Khatanga Gulf. The Khatanga Gulf is 250 km long; its width is 25–50 km. The shallow (5–20 m deep) inner and deep (20–30 m deep) outer parts of the gulf are connected by a narrow strait (15–20 km wide) between the Khara-Tumus and Taymyr peninsulas (Fig. 1c). The Bolshoy Begichev Island is located in the outer part of the Khatanga Gulf and divides it into two straits. The southern strait is narrow (8 km wide) and shallow (10 m deep), while depth of the northern strait (15–20 km wide) between the Bolshoy Begichev Island and the Taymyr Peninsula steadily increases towards the open sea to 25–30 m and connects the Khatanga Gulf with the western part of the Laptev Sea. The Khatanga Gulf is covered by ice in October – July. Tides in the Khatanga Gulf are among the largest in the Eurasian part of the Arctic Ocean. Maximal tidal range in different part of the gulf is 1–2 m [Pavlov et al., 1996; Kulikov et al., 2018]. The largest tidal velocities up to 1.4–1.7 m/s were registered at the straits that connect the outer part of the gulf with the inner part and the open sea, which are described above [Korovkin and Antonov, 1938; Pavlov et al., 1996].~~

~~3 Data~~

~~**Hydrographic in situ data used in this study were collected during three oceanographic field surveys in the Kara and Laptev seas including the 4th cruise of the R/V "Nikolay Kolomeytsev" on 27–29 August 2000 in the south-western part of the Laptev Sea, the 66th cruise of the R/V "Akademik Mstislav Keldysh" on 24–26 July 2016 in the Yenisei Gulf and the central part of the Kara Sea, the 69th cruise of the R/V "Akademik Mstislav Keldysh" on 17–18 September 2017 in the Khatanga Gulf and the western part of the Laptev Sea (Fig. 1). Field surveys included continuous measurements of salinity in the surface sea layer (2–3 m depth) performed at 100 m spatial resolution along the ship track using a ship board pump-through system equipped by a conductivity-temperature-depth (CTD) instrument (*Sea-Bird Electronics SBE 21 SeaCAT Thermosalinograph*) [Zavialov et al., 2015; Osadchiev et al., 2017]. Vertical profiles of salinity were performed using a CTD instrument (*Sea-Bird Electronics SBE 911plus CTD*) at 0.2 m vertical resolution. This CTD profiler was equipped with two parallel temperature and conductivity sensors; the mean temperature differences between them did not exceed 0.01°C, while differences of salinity were not greater than 0.01. Discharge data used in this study was obtained at the most downstream gauge stations at the Yenisei and Khatanga rivers located approximately 650 and 200 km far from the river mouths, respectively.~~**

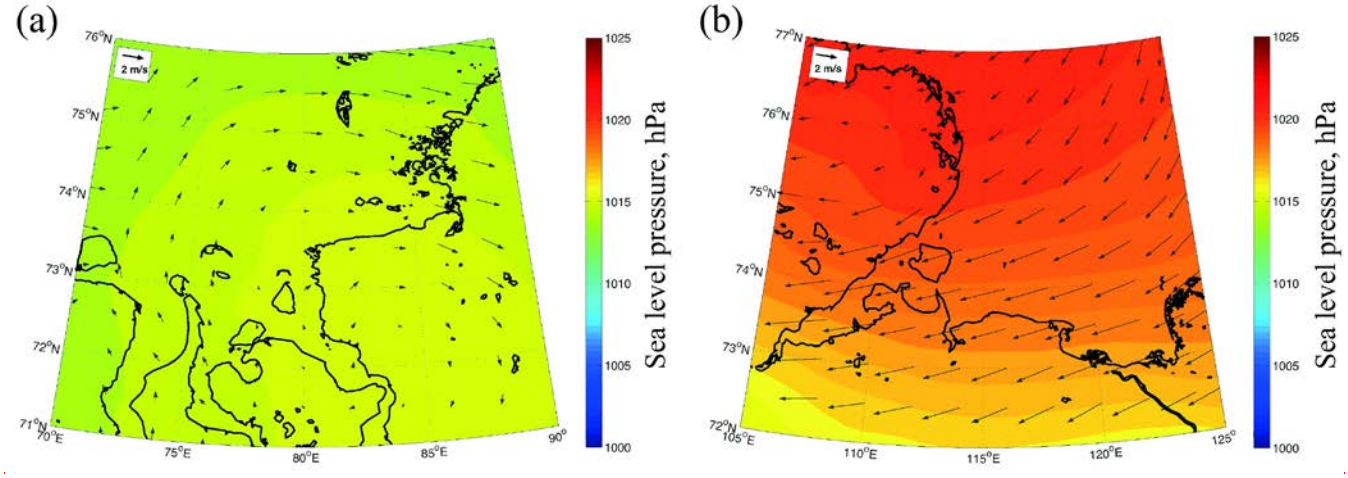

~~Figure 2: Average wind forcing (arrows) and sea level pressure (color) during 12-26 July 2016 in the central part of the Kara Sea (a) and during 24-18 September 2017 in the western part of the Laptev Sea (b) obtained from ERA5 atmospheric reanalysis.~~

~~4~~ 3 Results

3.1 Tidal forcing in the Yenisei and Khatanga gulfs

To study tidal forcing in the Yenisei and Khatanga gulfs we analysed in situ measurements of sea level performed at three tide gauges, namely: Leskin and Dikson in the Yenisei Gulf (Fig. 1b), Preobrazheniye in the Khatanga Gulf (Fig. 1c). These measurements were performed every hour during summer and autumn at the Leskin station (1977 – 1979, 1981 – 1992) and during the whole year at the Dikson (1977 – 1979, 1981 – 1990) and Preobrazheniye (1978 – 1979, 1981 – 1988) stations. The tidal harmonic constants were calculated from these data by the *Matlab* harmonic analysis toolbox *T_Tide* [Pawlowicz et al., 2002]. We analysed time series during the period of one year and then estimated the vector averaged amplitudes to obtain the mean long-term values of the amplitudes of the tidal harmonics [Medvedev et al. 2013]. As a result, we estimated amplitudes of 68 tidal constituents for the Dikson and Preobrazheniye stations, as well as amplitudes of 35 or 50 tidal constituents (for different years) for the Leskin station. We revealed that tidal circulation in the study areas is dominated by the main semidiurnal tidal constituent (M_2) and is also affected by the S_2, K_1, and O_1 constituents, while the role of the other tidal harmonics is insignificant. The obtained mean amplitudes of four major tidal constituents and the mean spring tidal ranges at the considered stations are presented in Table 1.

Table 1: The mean amplitudes of four major tidal constituents and the mean spring tidal ranges reconstructed for the Leskin, Dikson, and Preobrazheniye tide gauge stations.

Tidal gauge stations	Mean amplitudes, cm				Mean spring tidal ranges, cm
	M_2	S_2	K_1	O_1	
Leskin	16.0	7.3	3.4	1.7	46.5
Dikson	8.2	3.9	1.9	1.2	24.2
Preobrazheniye	35.1	15.1	5.0	2.7	100.2

The smallest mean amplitudes of the main tidal harmonic M_2 and mean spring tidal ranges ($2M_2 + 2S_2$) are observed at the Dikson station (8.2 and 24.2 cm) at the mouth of the Yenisei Gulf. The mean tidal amplitudes and ranges are twice large (16.0 and 46.5 cm) in the Leskin station between the inner and outer parts of the Yenisei Gulf, and four times large (35.1 and 100.2 cm) at the Preobrazheniye station at the mouth of the Khatanga Gulf, as compared to the Dikson station. These results are in good agreement with previous assessments of tidal forcing in the Yenisei and Khatanga gulfs [Voinov, 2002; Korovkin and Antonov, 1938] and demonstrate that tidal forcing in the Khatanga Gulf is significantly stronger than in the Yenisei Gulf. Moreover, Korovkin and Antonov [1938] reported that tidal forcing intensifies in the outer part of the Khatanga Gulf. In situ measurements performed in August 1934 showed that the amplitude of M_2 increased from 42 cm near

the Preobrazheniye Island (where the Preobrazheniye station is located) to 50 cm at the western shore of the Bolshoy Begichev Island and to 83 cm near the Khara-Tumus Peninsula (that separates the inner and outer parts of the gulf) [Korovkin and Antonov, 1938]. The registered spring tidal range near the western shore of the Bolshoy Begichev Island was 150 cm and increased to 259 cm near the Khara-Tumus Peninsula.

The amplitude of M_2 and spring tidal range at the Preobrazheniye station have large seasonal and inter-annual variability caused by variability of river discharge and ice coverage. In particular, the reconstructed mean annual amplitudes of M_2 varied from 32 to 42 cm, while the mean monthly spring tidal range varied from 87 cm in May to 130 cm in August [Kulikov et al., 2020]. Therefore, in order to analyse influence of tidal mixing on structure and spreading of the Yenisei and Khatanga plumes during the periods of field measurements addressed in this study, we reconstructed velocities of tidal currents in the Yenisei Gulf in July 2016 and in the Khatanga Gulf in September 2017 using the AOTIM5 tidal model (Fig. 2). Voinov [2002] reported that maximal velocities of tidal currents in the Yenisei Gulf in summer are equal to 30–40 cm/s in the outer part of the gulf along the Taymyr Peninsula. The modelled maximal tidal velocities in July 2016 were equal to 10-20 cm/s in the inner part of the estuary and up to 25 cm/s in the outer part of the estuary (Fig. 2a). Modelled maximal tidal velocities in the Khatanga Gulf were much larger than in the Yenisei Gulf and increased from 20–50 cm/s in the outer part of the estuary to 80–100 cm/s in the inner part of the estuary (Fig. 2a).

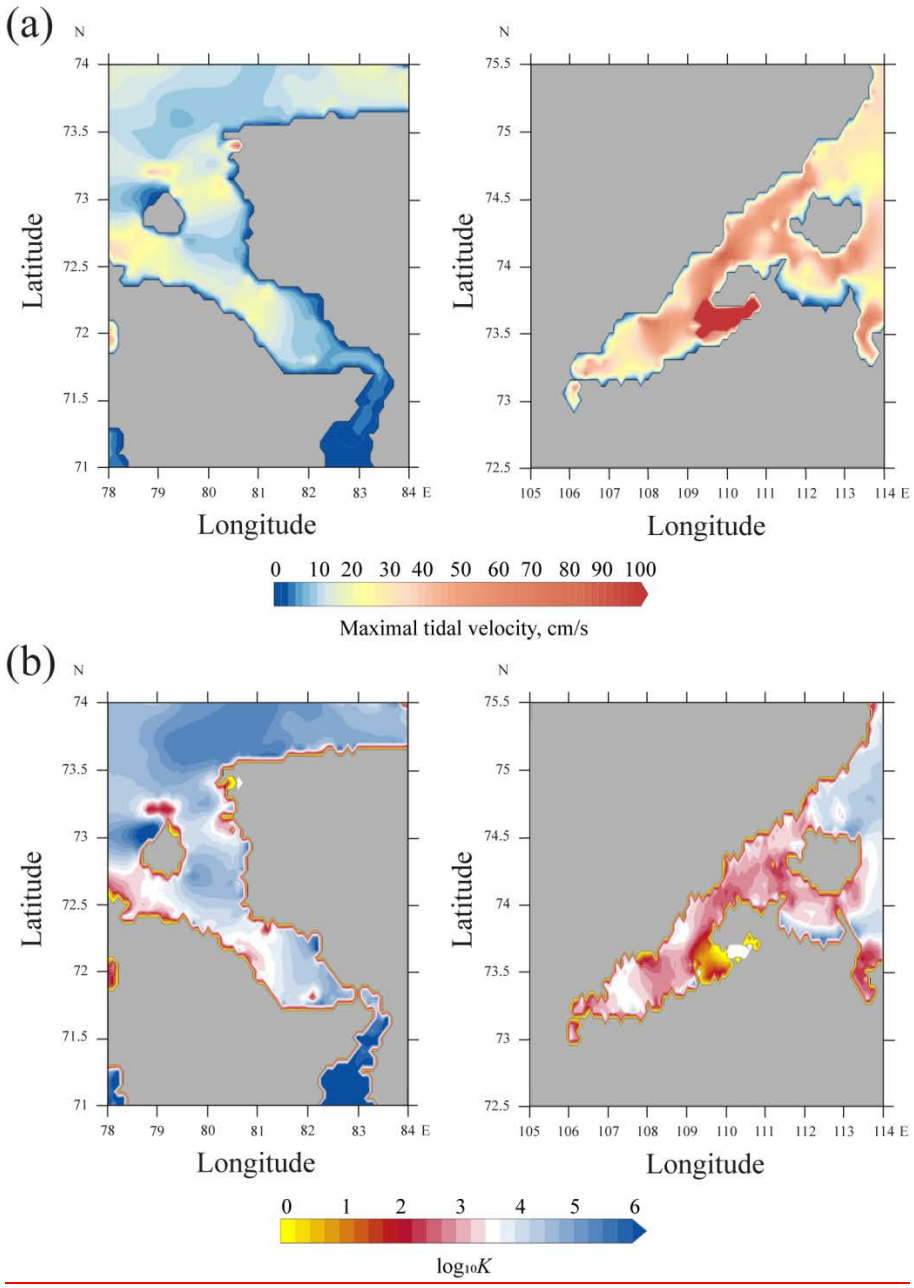

Figure 2: Distributions of maximal tidal velocity (a) and common logarithm of the Hunter-Simpson parameter *K* (b) in the Yenisei (left) and Khatanga (right) gulfs.

Basing on tidal data simulated by AOTIM5 model and IBCAO bathymetric data we calculated distribution of the Simpson-Hunter parameter $K = h / U^3$, where h is the sea depth and U is the average tidal velocity [Simpson and Hunter, 1974]. This parameter is indicative of intensity of tidal-induced mixing of water column [Simpson and Hunter, 1974; Garrett et al., 1978] and was used in many studies for identification of sea areas where tidal-induced turbidity penetrates from sea bottom to the

surface layer [Chen et al., 2009; Korotenko et al., 2014]. In this study we used tidal velocities averaged in the Yenisei Gulf during July 2016 and in the Khatanga Gulf during September 2017 in the following way: $\bar{U} = \langle\sqrt{(u^2 + v^2)}\rangle$, where u and v are the time series of the north and east components of the tidal currents reconstructed from the eight tidal constituents. Due to wide ranges of variability of K in the Yenisei and Khatanga gulfs we analyzed its common logarithm $\log_{10}(K)$ which distribution is shown in Fig. 2b. The value of $\log_{10}(K)$ is relatively small (3.5–5) in the Yenisei Gulf that shows low influence of tides on estuarine mixing in the surface layer. In contrast to the Yenisei Gulf, the value of $\log_{10}(K)$ is near 1.5–3 within the majority of area of the Khatanga Gulf that indicates extremely intense tidal-induced mixing in this area (Fig. 2b).

3.2 Wind forcing in the Kara and Laptev seas

Using the ERA5 atmospheric reanalysis, we studied influence of wind forcing on the Yenisei and Khatanga plumes during the periods preceding in situ measurements in 2016 and 2017. For this purpose, we reconstructed daily averaged wind speed and direction during 29 June – 26 July 2016 in the central part of the Kara Sea (Fig. 3) and during 8 August – 18 September 2017 in the southwestern part of the Laptev Sea (Fig. 4). These wind time series cover ice-free periods at the study areas from decline of ice coverage to in situ measurements in the Yenisei and Khatanga plumes, i.e., the periods when wind forcing affected spreading of the river plumes.

Wind forcing in the central part of the Kara Sea was weak and moderate for the majority of days during 29 June – 26 July 2016 (Fig. 3). Daily averaged values of wind speed at the study area varied between 1 and 9 m/s, while their mean value was 4 m/s (Fig. 3b). On 10-13 July 2016, i.e., during 4 days, the longest continuous period of strong winds (> 5 m/s) was observed in the central part of the Kara Sea. Moreover, the direction of predominant winds showed significant synoptic variability during the considered period due to high variability of atmospheric pressure. As a result, wind forcing averaged during 2-week time periods is characterized by even more low wind speed, namely, < 4 m/s during 29 June – 11 July and < 2 m/s during 12-26 July, (Fig. 3a).

~~Wind forcing during several weeks preceding in situ measurements in July 2016 in the Kara Sea and in September 2017 in the Laptev Sea was weak and moderate (Fig. 2). No storm events occurred during this period in the study areas, average wind speed was <4 m/s in the central part of the Kara Sea and <7 m/s in the western part of the Laptev Sea.~~

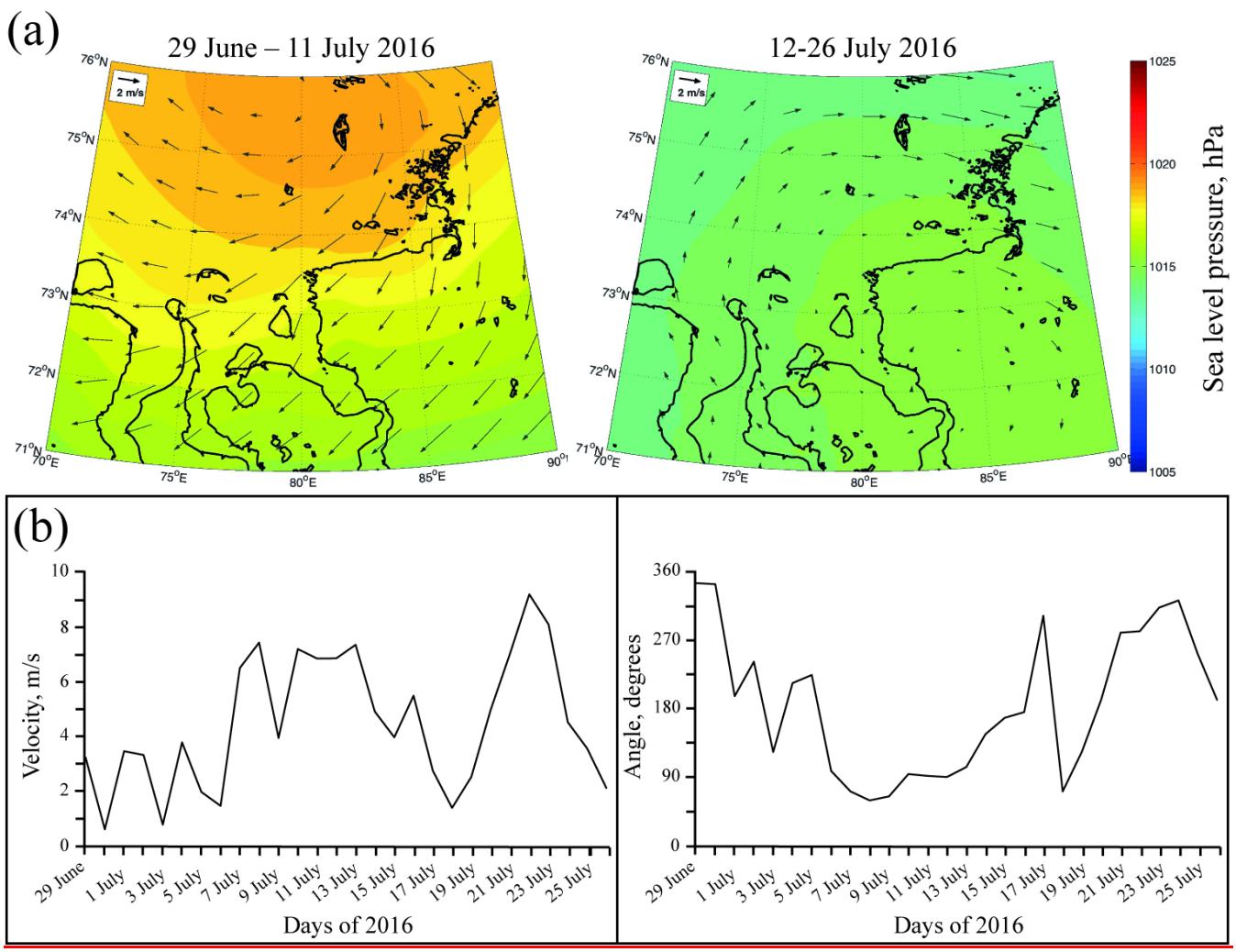

Figure 3: Average wind forcing (arrows) and sea level pressure (color) during 29 June – 11 July (left) and 12-26 July 2016 (right) in the central part of the Kara Sea (a). Daily average wind speed (left) and direction (right) during 29 June – 26 July 2016 obtained from ERA5 atmospheric reanalysis. Wind data were obtained from the ERA5 atmospheric reanalysis.

Similarly to the central part of the Kara Sea in July 2016, wind forcing in the southwestern part of the Laptev Sea was mainly low/moderate and highly variable during 8 August – 18 September 2017 (Fig. 4). No storm events occurred during this period, daily averaged values of wind speed varied between 1 and 8 m/s, while their mean value was 4 m/s (Fig. 4b). The longest continuous period of strong wind forcing lasted only during 3 days (6-8 September 2017). Atmospheric circulation in the southwestern part of the Laptev Sea was dominated by multiple cyclones and anticyclones during the considered period. Due to the observed intraday variability of predominant wind direction, speed of 2-week averaged wind forcing was < 2 m/s during 8-21 August 2017 and was < 4 m/s during 22 August – 3 September and 4-18 September 2017 (Fig. 4a).

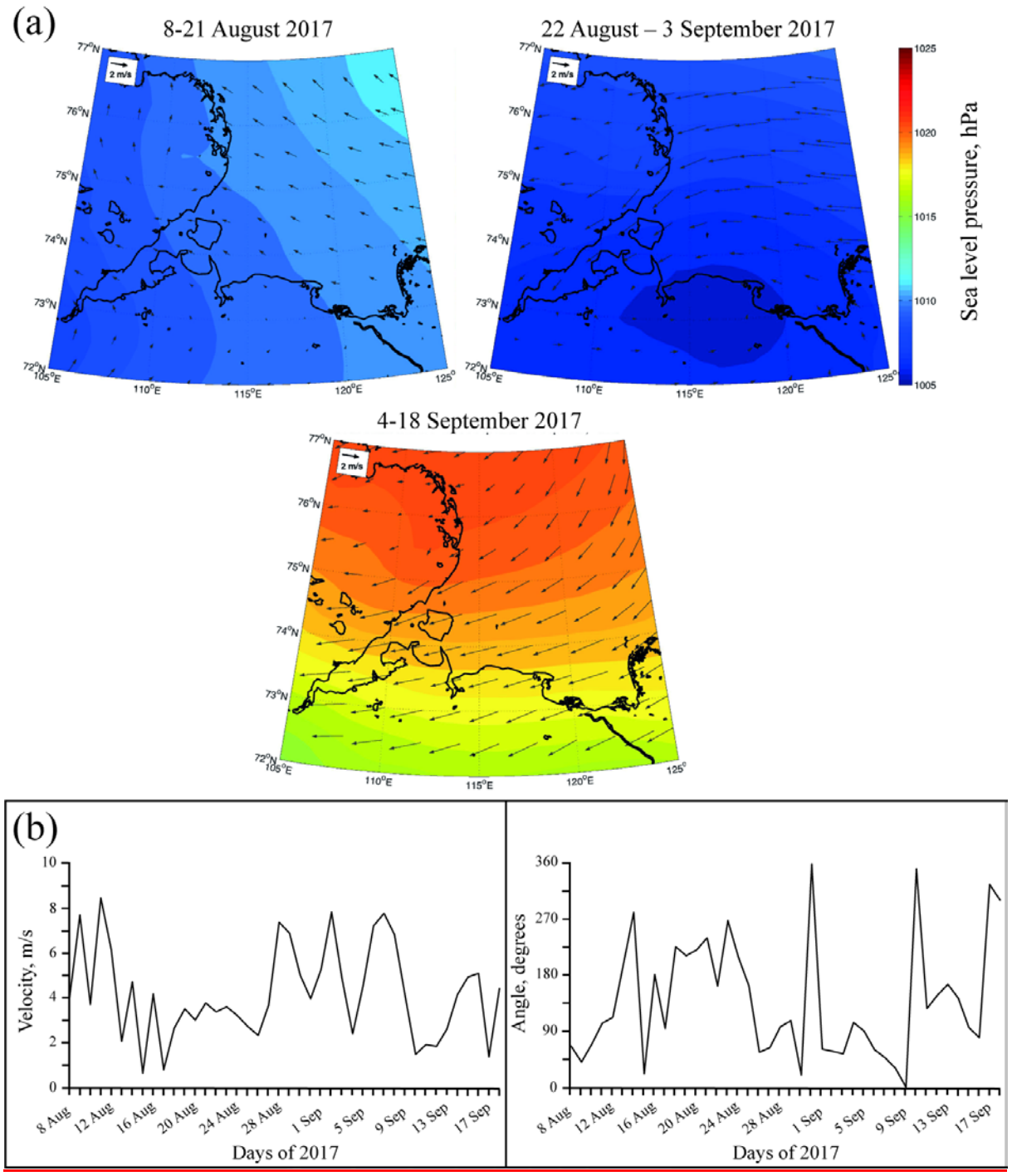
(a)
8-21 August 2017
22 August – 3 September 2017
4-18 September 2017
2 m/s
77°N
76°N
75°N
74°N
73°N
72°N
105°E
110°E
115°E
120°E
125°
1025
1020
1015
1010
1005
Sea level pressure, hPa
(b)
Velocity, m/s
Angle, degrees
360
270
180
90
0
10
8
6
4
2
8 Aug
12 Aug
16 Aug
20 Aug
24 Aug
28 Aug
1 Sep
5 Sep
9 Sep
13 Sep
17 Sep
Days of 2017

Figure 4: Average wind forcing (arrows) and sea level pressure (color) during 8-21 August (top left), 22 August – 3 September (top right), and 4-18 September 2017 in the western part of the Laptev Sea (a). Daily average wind speed (left) and direction (right) during 8 August – 18 September 2017. Wind data were obtained from the ERA5 atmospheric reanalysis.

3.3 Vertical salinity structure of the Yenisei and Khatanga plumes

The in situ measurements performed in July 2016 in the Kara Sea during the period of peak discharge of the Yenisei River (approximately 30~~-~~000 m^3/s) revealed that the Yenisei plume was spreading more than 500 km northward from the river mouth and its depth and vertical structure did not change much along this distance (Fig. ~~3a~~5a). The Yenisei plume occupied the whole water column in the shallow inner part of the estuary, its surface salinity was 0-5 (stations 5341-5345). Further northward the plume detached from the sea bottom. The plume depth (defined by the isohaline of 25) remained equal to 8-12 m in the outer part of the estuary (stations 5337-5340 and 5348) and at the Kara Sea shelf (stations 5333-5336 and~~-~~ 5349-5350). Surface salinity of the plume also was relatively stable and slowly increased from 6 to 10 in this 300 km long part of the transect. Sharp salinity gradient was observed between the plume and the subjacent sea, vertical distance between the isohalines of 10 and 25 ~~did not exceed several~~was 2-5 meters. Further northward surface salinity abruptly increased from 15 (station 5351) to 28 (station 5352) in a distance of 10 km indicating the northern boundary of the Yenisei plume.

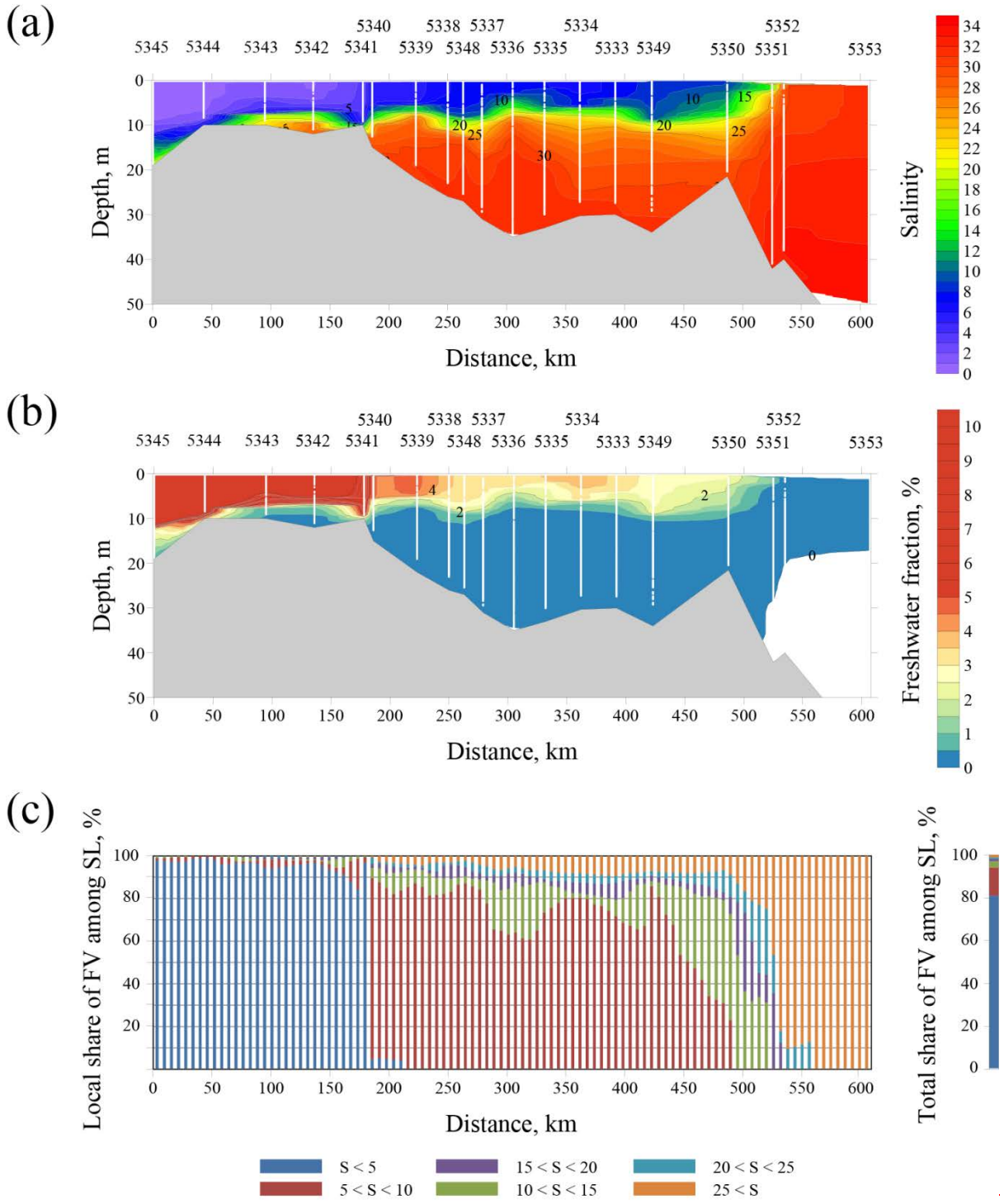

Figure 3: The vertical salinity structure (a), distribution of freshwater fraction (b), local and total shares of freshwater volume (FV) among salinity layers (SL) in water column (c) along the ship track in the Yenisei Gulf and the adjacent shelf of the Kara Sea on 24-26 July 2016.

~~According to Nash et al. [2009],~~In order to quantify the effect of estuarine mixing on the Yenisei plume, we calculated vertical distribution of freshwater fraction $F = (S_0 - S) / S_0$ along the transect (Fig. ~~3b~~5b), where S is the observed salinity, S_0 is the reference ambient sea salinity prescribed equal to 32. F ~~represents~~ is equal to the ratio between the volumes of river water and sea water that were mixed and produced the observed salinity in the water parcel ~~the volume fraction of freshwater in~~of the Yenisei plume ~~that produced the observed salinity after being mixed with ambient sea water~~. The value of the reference salinity equal to 32 was chosen according to typical salinity of ambient sea water at the shelves of the central part of the Kara Sea and the south-western part of the Laptev Sea [Pavlov et al., 1996; Johnson et al., 1997; Williams and Carmack, 2015]. In order to assess the process of dilution of freshwater discharge within the Yenisei plume, we defined five different salinity ranges of the river plume water, namely, $0 < S < 5$, $5 < S < 10$, $10 < S < 15$, $15 < S < 20$, $20 < S < 25$, as well as the salinity range $S > 25$ for the ambient sea. Then for all vertical salinity profiles of the transect we calculated the local shares of freshwater volume in water column among these salinity ranges, i.e., what percentage of total freshwater volume contained in the water column is located between the isohalines of 0 and 5 (salinity range of 0-5), between the isohalines of 5 and 10 (salinity range of 5-10), etc. (Fig. 5c). Finally, we calculated the total shares of freshwater volume in water column among these salinity ranges by averaging the reconstructed local shares of freshwater volume along the transect (Fig. 5c).

Figure ~~3~~ 5 illustrates that the Yenisei discharge ~~exhibited~~ experienced relatively little mixing in the estuary due to weak tidal forcing. As a result, ~~the majority of~~ river runoff propagated off the estuary within the low-~~saline~~ salinity and shallow Yenisei plume (Fig. ~~3b~~5b). Strong stratification between the plume and the subjacent shelf sea hindered vertical mixing. Freshwater fraction remained concentrated in the shallow and low-~~saline~~ salinity surface layer in the open part of the Kara Sea till station 5350 located 500 km ~~far~~ from the river mouth. The majority of freshwater volume in water column was located in two salinity ~~layers~~ranges, namely, ~~between the isohalines of~~ in 0 ~~and~~ 5 salinity range ~~(~~in the inner estuary~~)~~ and ~~between the isohalines of~~in 5 ~~and~~ 10 salinity range ~~(~~in the outer estuary and at the sea shelf~~)~~ (Fig. ~~3c~~5c). ~~Salinity~~ As a result, ~~layers of~~ 0-5 and 5-10 salinity ranges accounted for 80% and 15% of total freshwater volume along the transect, respectively (Fig. ~~3c~~5c).

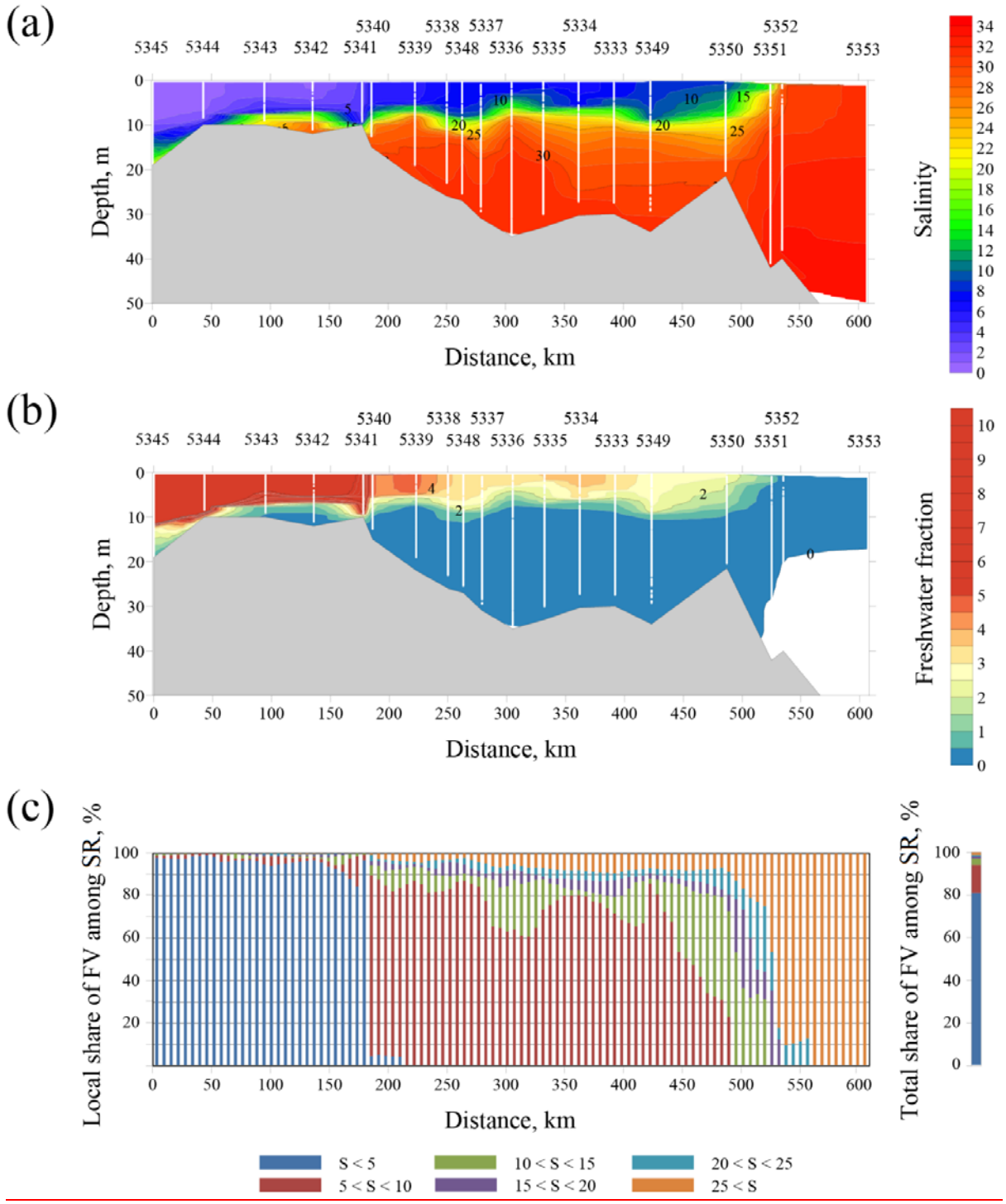

Figure 5: The vertical salinity structure (a), distribution of freshwater fraction (b), local and total shares of freshwater volume (FV) among salinity ranges (SR) in water column (c) along the ship track in the Yenisei Gulf and the adjacent shelf of the Kara Sea on 24-26 July 2016.

Despite low discharge rate of the Khatanga River (approximately 3~~-~~000 m^3/s) ~~during 17-18~~in September 2017, the horizontal extent of the Khatanga plume during 17-18 September 2017 was similar to that of the Yenisei plume, while its maximal depth even exceeded the depth of the Yenisei plume (Fig. ~~4a~~6a). The Khatanga plume was weakly-stratified and occupied the whole water column in the shallow inner part of the estuary (stations 5627-2629) due to intense tidal mixing in the Khatanga Gulf. Tidal-induced dilution caused increase of surface salinity and depth of the plume from 4 and 7 m (station 5628) to 17 and 25 m (station 5630) at 120 km along the transect. In the outer part of the estuary the plume detached from sea bottom and its depth steadily decreased to 11 m, while surface salinity increased to 21 (station 5632). Further northeastward at the Laptev Sea shelf the plume salinity slightly increased to 22, while depth slightly decreased to 9 m in a distance of 100 km from the Khatanga Gulf (station 5591). Distinct salinity gradient between the plume and the subjacent sea ~~was stable~~slightly changed along the northeastern part of the transect. Vertical distance between the isohalines of 25 and 30 ~~did not exceed several~~was 2-4 meters in the outer estuary and the ~~coastal~~ shelf sea. ~~Salinity measurements performed in the surface layer revealed that the boundary of the Khatanga plume was located further northward, approximately 250 km from the Khatanga Gulf and 500 km far from the river mouth (Fig. 5c).~~

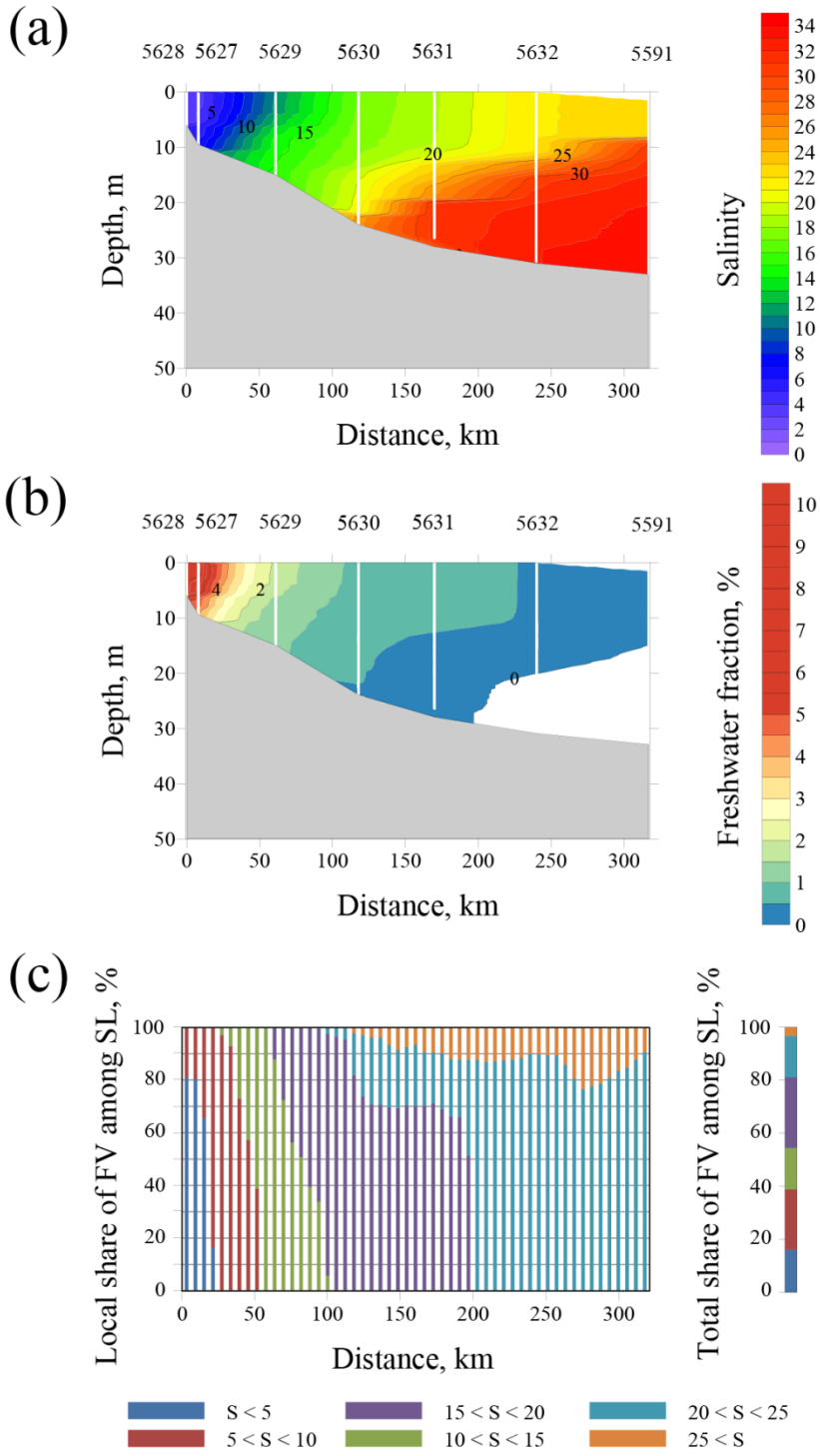

350 **Figure 4: The vertical salinity structure (a), distribution of freshwater fraction (b), local and total shares of freshwater volume (FV) among salinity layers (SL) in water column (c) along the ship track in the Khatanga Gulf and the adjacent shelf of the Laptev Sea on 17-18 September 2017.**

The Khatanga discharge ~~exhibited~~ experienced intense estuarine tidal mixing and, therefore, was distributed from surface to bottom in the inner estuary and over 20-25 m deep water column in the outer estuary (Fig. ~~4b~~6b). As a result, relatively small freshwater volume formed a deep, but diluted river plume. Salinity and freshwater fraction in the Khatanga plume ~~remained stables~~slightly changed while it was spreading from the estuary to the open part of the Laptev Sea. Freshwater volume in the water column steadily transferred from 0-5 salinity ~~layer~~ range ~~of 0-5~~ near the river mouth to 20-25 salinity ~~layer~~ range ~~of 20-25~~ in the open sea (Fig. ~~4c~~6c). Total freshwater volume along the transect was almost homogenously distributed among salinity ~~layers~~ ranges of 0-5, 5-10, 10-15, 15-20, and 20-25 (Fig. ~~4c~~6c). ~~Thus, the Khatanga plume was formed by relatively small volume of freshwater discharge, however, mixed with large volume of saline water in the estuary that is indicated by low freshwater fraction in the plume. As a result, the Khatanga plume occupied large volume and area at the Laptev Sea. In particular, surface salinity in the southwestern part of the Laptev Sea remained less than 25 at a distance of 250 km from the Khatanga Gulf (Fig. 5c).~~

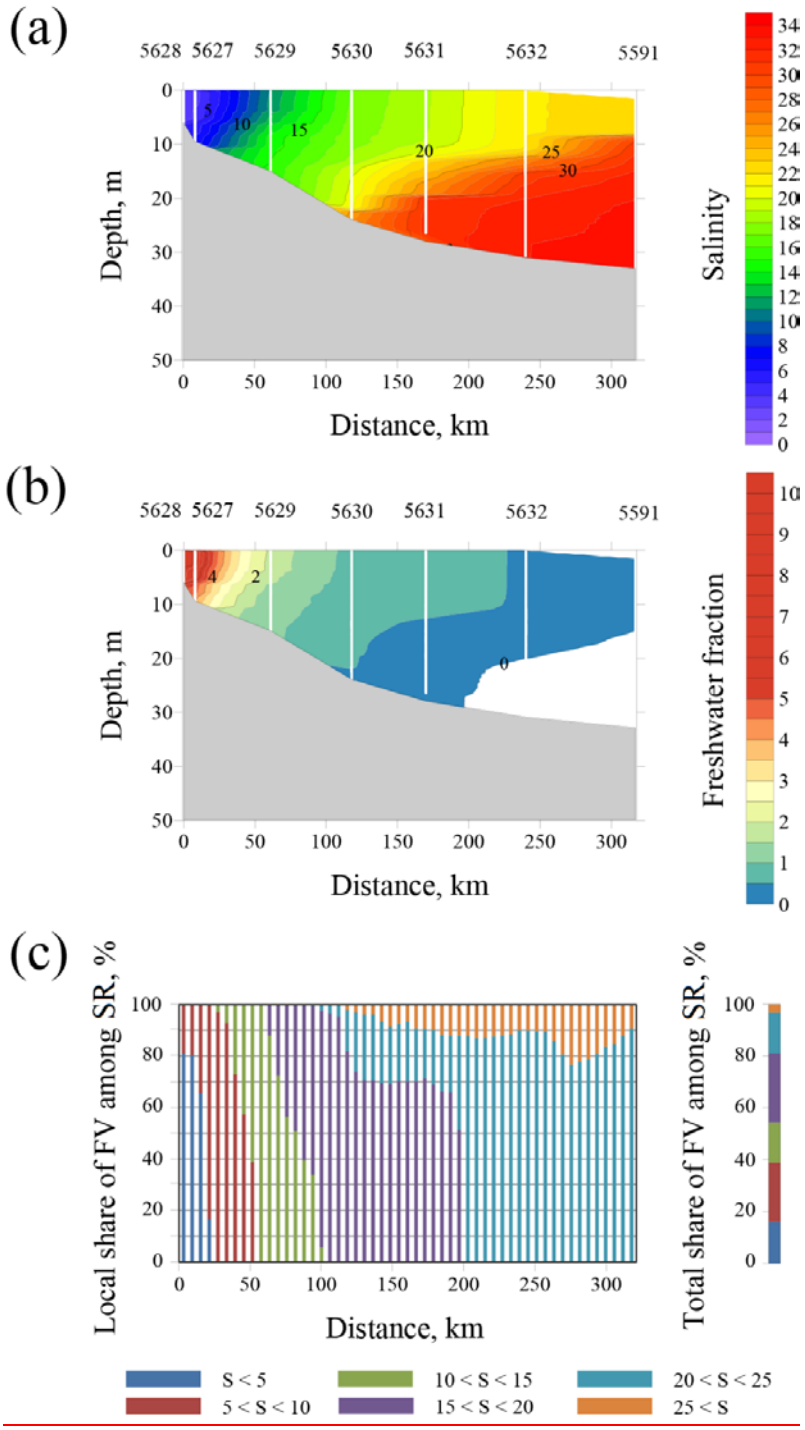

365 **Figure 6: The vertical salinity structure (a), distribution of freshwater fraction (b), local and total shares of freshwater volume (FV) among salinity ranges (SR) in water column (c) along the ship track in the Khatanga Gulf and the adjacent shelf of the Laptev Sea on 17-18 September 2017.**

3.4 Spatial extents of the Yenisei and Khatanga plumes

In order to assess and compare spatial extents of the Yenisei and Khatanga plumes, we analysed in situ salinity measurements in the surface layer performed in the Kara and Laptev seas during field surveys referred above (Fig. 7), as well as satellite observations of the study areas in 2000-2019 (Fig. 8-10). Continuous surface salinity measurements along the ship track detected the border of the river plume in the central part of the Kara Sea in July 2016 defined by the isohaline of 25 (Fig. 7a). This buoyant plume was formed by discharges of the Ob and Yenisei rivers, i.e., river runoff from the closely located Ob and Yenisei gulfs formed the Ob and Yenisei plumes that coalesced into the joint Ob-Yenisei plume [Pavlov et al., 1996; Zatsepin et al., 2010; Zavialov et al., 2015].

The ship track in July 2016 crossed twice the northern boundary of the Ob-Yenisei plume at the meridional transects from the Ob and Yenisei gulfs (Fig. 7a). Surface salinity measurements along the other segments of the ship track showed absence of the Ob-Yenisei plume in the western and northern parts of the Kara Sea. However, the detailed location of the boundary of the Ob-Yenisei plume was not detected. Also, the performed salinity measurements did not distinguish the western part of the Ob-Yenisei plume formed by the Ob discharge and the eastern part of the Ob-Yenisei plume formed by the Yenisei discharge. These drawbacks of in situ measurements were substituted by satellite observations of the study area.

Due to common cloudy weather conditions in the Kara Sea, we analysed the satellite imagery of the study area acquired on 15 July 2016 when the Ob-Yenisei plume was clearly seen in optical satellite images and the structure of surface turbidity, temperature, and chlorophyll-a could be identified (Fig. 8). Satellite Chl-a distribution in the Kara Sea reveals location of the border of the Ob-Yenisei plume (Fig. 8c) which is in a very good accordance with in situ salinity measurements performed 9-11 days after the satellite observations (Fig. 7a). Significant differences in temperature and concentration of suspended sediments in the Ob (10-12 °C and 40 g/m^3) and Yenisei (16-18 °C and 10 g/m^3) river water [Gordeev et al., 1996] provides opportunity to distinguish the Ob- and Yenisei-dominated parts of the Ob-Yenisei plume.

CR (Fig. 8a) and BT (Fig. 8b) satellite products show, first, the meandering turbid and cold jet from the Gulf of Ob that forms the relatively small western Ob-dominated part of the Ob-Yenisei plume and, second, the low-turbid and warm jet from the Yenisei Gulf that forms the large warm and low-turbid eastern Yenisei-dominated part of the Ob-Yenisei plume. The observed difference in areas of the Ob- and Yenisei-dominated parts is caused by different discharge regimes of the Ob and Yenisei rivers. The discharge rate of the Yenisei River has distinct freshet peak in June – July, while the discharge rate of the Ob River is characterised by steady increase and decrease of discharge in May – September [Pavlov et al., 1996; Osadchiev et al., 2017]. As a result, the freshwater runoff from the Yenisei River in June – July (~ 120 m^3/s) is twice greater than that from the Ob River (~ 60 m^3/s). Therefore, based on the joint analysis of in situ and satellite data, we detected the spreading area of the Yenisei plume in July 2016 and revealed that its boundary was located 200-250 km from the Yenisei Gulf.

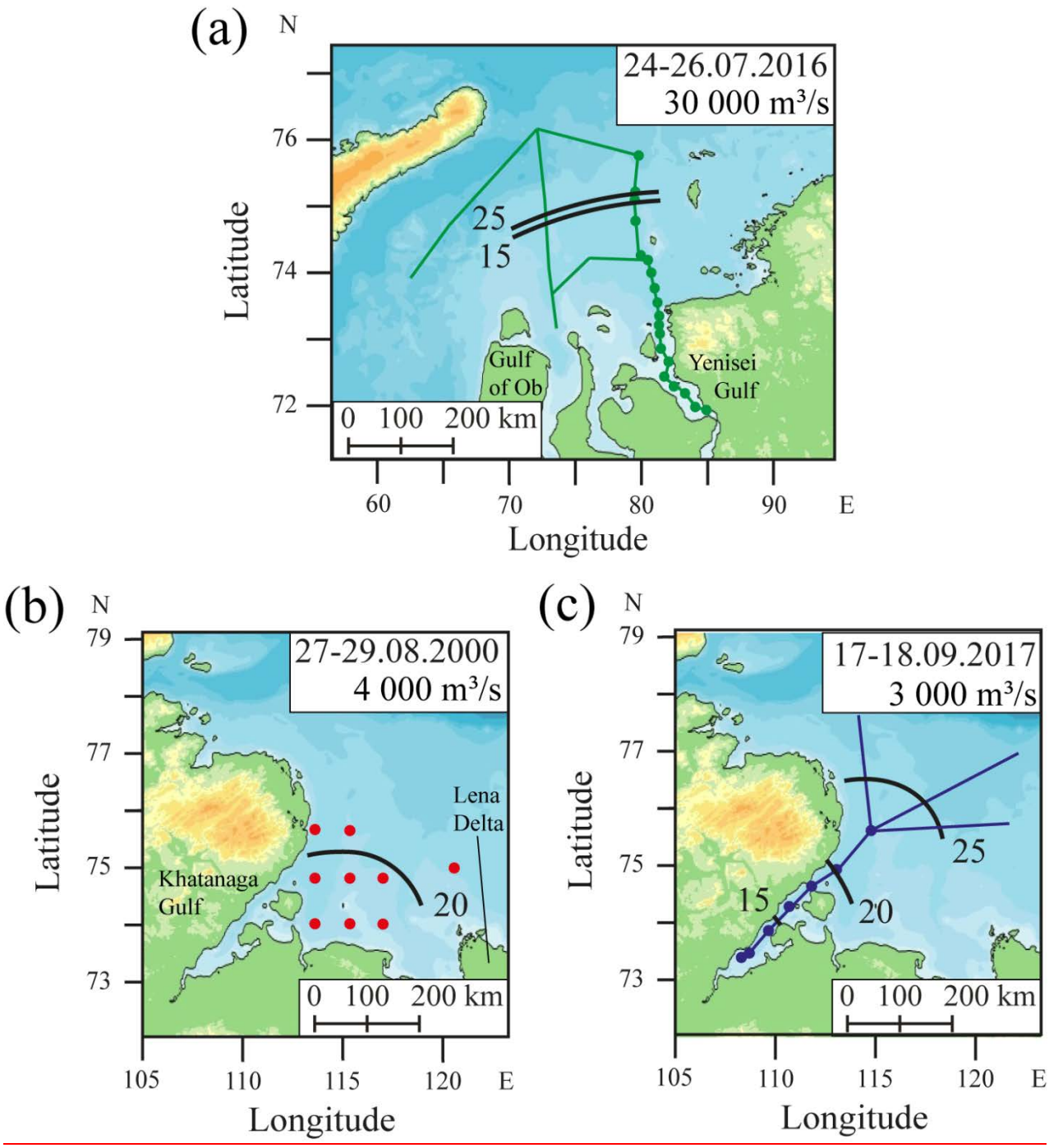

400 **Figure 7: Location of the isohalines of 15, 20, and 25 at the surface layer (black lines) at the central part of the Kara Sea (a) and the western part of the Laptev Sea (b, c) indicating spatial scales of the Ob-Yenisei (a) and Khatanga (b, c) river plumes reconstructed from in situ measurements conducted in August 2000 (red) and September 2017 (blue) in the Laptev Sea and in July 2016 (green) in the Kara Sea. The dates of the field measurements and the discharge rates of the rivers during these periods are shown at the figures. The graphic scales correspond to the latitude of 73°.**

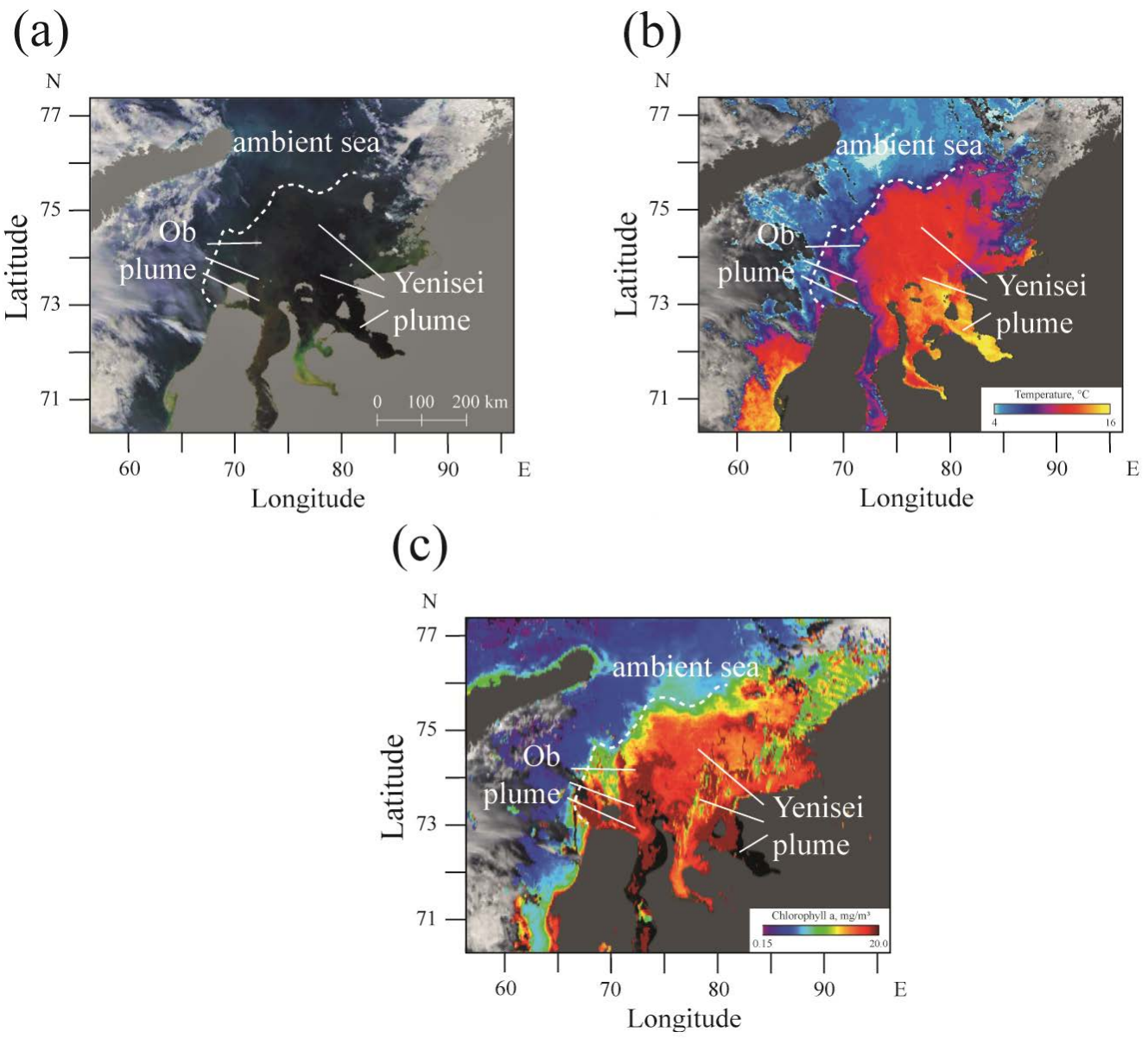

Figure 8: Corrected reflectance (a), brightness temperature (b), and concentration of chlorophyll-a (c) from MODIS Aqua satellite image of the central part of the Kara Sea acquired on 15 July 2016.

Unlike the Ob-Yenisei plume formed by discharges of two large rivers, the Khatanga River is the only large river that forms the buoyant plume in the southwestern part of the Laptev Sea. The Lena River is the closest large river to the Khatanga Gulf that inflows to the Laptev Sea. However, the distance between the Khatanga Gulf and the Lena Delta is > 350 km (Fig. 7b). Moreover, 80-90% of large freshwater discharge from the Lena River (530 km^3 annually or 16800 m^3/s on average) inflows to the Laptev Sea from the eastern part of the Lena Delta, while its western part accounts only for 6-10% [Fedorova et al.,

2012]. As a result, the large Lena plume is formed in the central and southeastern parts of the Laptev Sea, in particular, it does not spread westward from the 120° E longitude to the southwestern parts of the Laptev Sea and does not merge with the Khatanga plume [Fofonova et al., 2015].

Continuous surface salinity measurements along the ship track in the southwestern part of the Laptev Sea detected the northern and northeastern segments of the border of the Khatanga plume in September 2017 (Fig. 7c). Surface salinity remained less than 25 at a distance of 200-250 km from the Khatanga Gulf and 450-500 km from the Khatanga River mouth. Another field survey conducted at the southwestern part of the Laptev Sea in the end of August 2000 also showed large spatial extents of the Khatanga plume (Fig. 7b). Distinct location of the plume boundary was not detected during this field survey due to absence of continuous measurements of surface salinity. However, the vertical profiles of salinity obtained at the hydrological stations showed that the isohaline of 20 in the surface layer was located at a distance of 50-200 km from the Khatanga Gulf.

Satellite observations of the study area acquired in the end of August 2000 confirmed the assessment of the spreading area of the Khatanga plume based on in situ measurements at the hydrological stations (Fig. 9). The Khatanga plume is characterized by elevated concentrations of suspended sediments and chlorophyll-a, as compared to the ambient saline sea. As a result, spreading area of the plume can be detected at cloud-free and ice-free CR and Chl-a satellite images of the study area. BT satellite products, on the opposite, are not effective for detection of the Khatanga plume due to relatively small difference between temperature in the diluted Khatanga plume and the ambient sea. Joint analysis of CR and Chl-a satellite images revealed that the border of the Khatanga plume on 23 and 25 August 2000 (a week after ice melting and 4 days before in situ measurements in the study area) was located at a distance of 50-250 km from the Khatanga Gulf which is consistent with in situ measurements. The region of elevated turbidity and elevated concentration of chlorophyll-a located eastward from the 120° E longitude and adjacent to the Lena Delta is associated with the western part of the Lena plume.

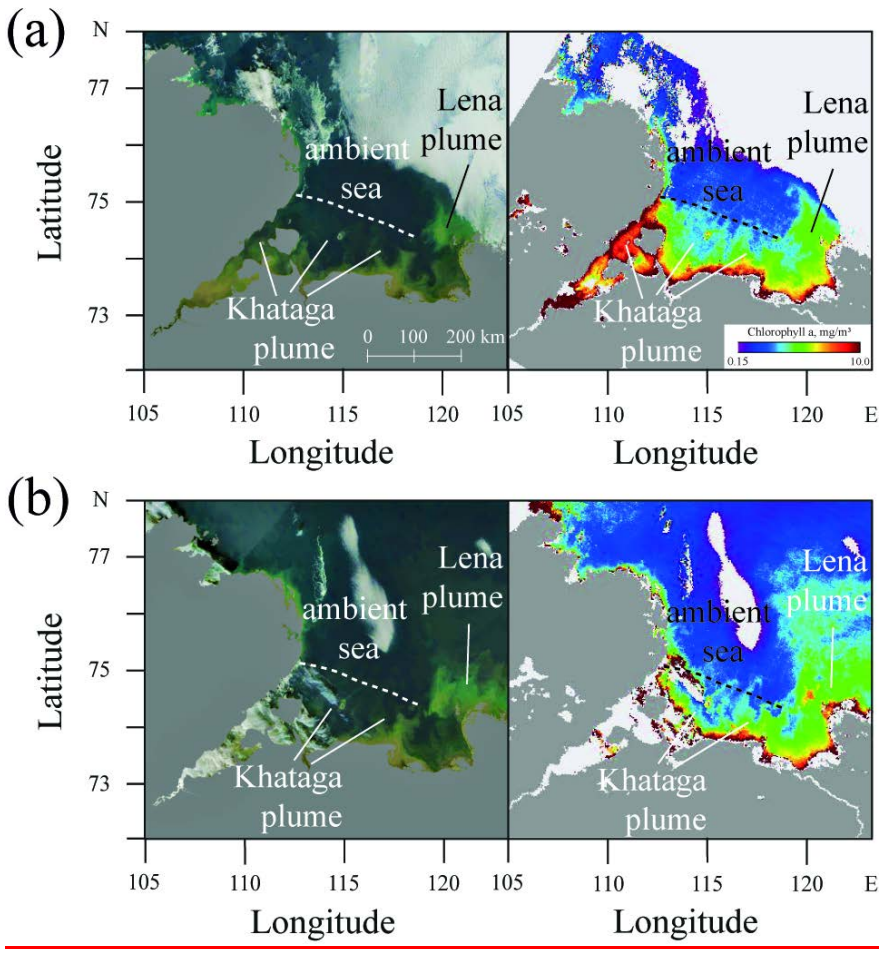

435 **Figure 9: Corrected reflectance (left) and concentration of chlorophyll-a (right) from MODIS Terra satellite images of the western part of the Laptev Sea acquired on 23 September (a) and 25 September (b) 2000.**

Constantly overcast sky at the southwestern part of the Laptev Sea in summer and autumn of 2017 hindered satellite observations of the Khatanga plume that could support the in situ measurements on 17-18 September 2017. However, the Khatanga plume was regularly observed at cloud-free images of the study area acquired in 2000-2019. In particular, the 440 spreading area and the boundary of the Khatanga plume are distinctly visible at several CR and Chl-a satellite images acquired during days when the whole southwestern part of the Laptev Sea was free of clouds (Fig. 10). Satellite observation showed significant variability of position and shape of the Khatanga plume border presumably associated with variability of external wind forcing. Wind-induced resuspension of bottom sediments that regularly occurs over shallow coastal areas between the Khatanga Gulf and the Lena Delta often hinders precise detection of the southeasternmost segment of the 445 Khatanga plume border. Nevertheless, satellite observations revealed that the Khatanga plume regularly occupied large area in the southwestern part of the Laptev Sea adjacent to the Khatanga Gulf. Maximal spatial extent of the Khatanga plume observed at satellite imagery in 2000-2019 varied between 150 and 250 km from the Khatanga Gulf.

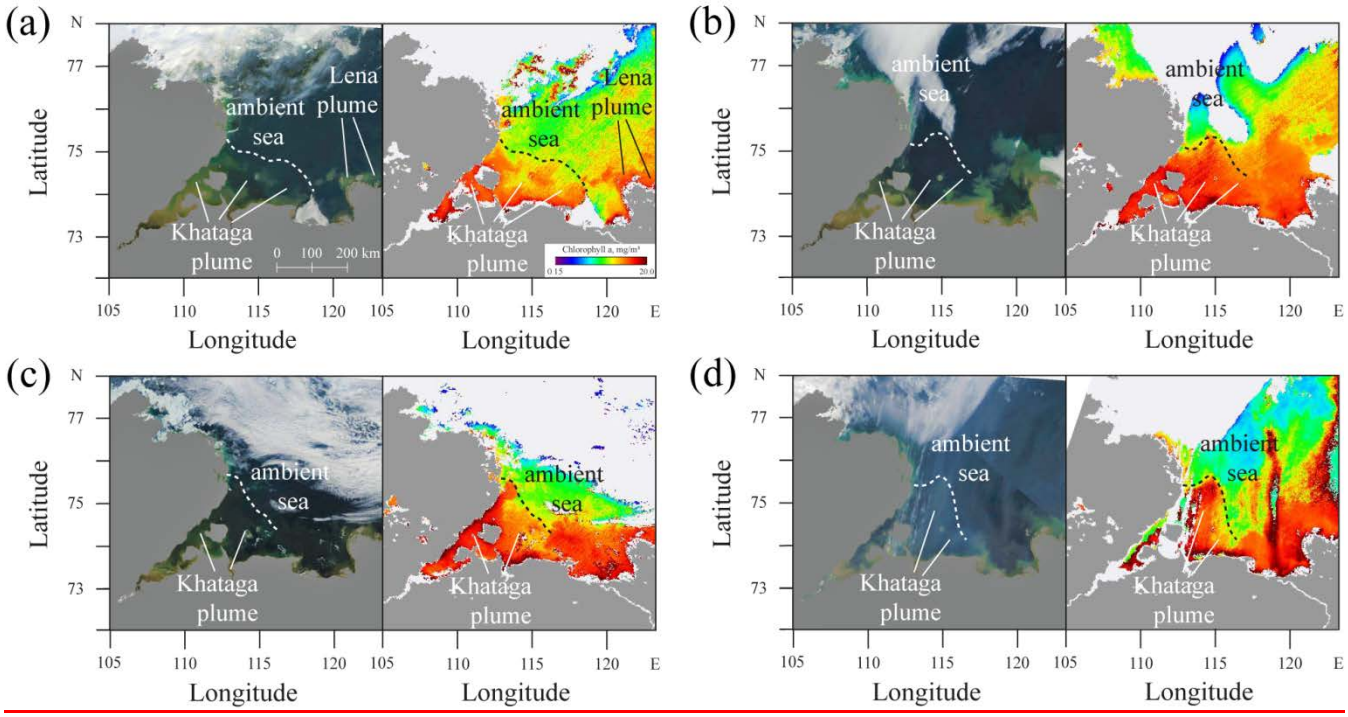

Figure 10: Corrected reflectance (left) and concentration of chlorophyll-a (right) from MODIS Terra and MODIS Aqua satellite images of the western part of the Laptev Sea acquired on 8 August 2003 (a), 13 August 2011 (b), 8 August 2013 (c), and 3 August 2019 (d).

~~5~~ 4 Discussion ~~and Conclusions~~

River discharge rate, wind forcing, and tidal circulation are the main factors that determine estuarine circulation and govern vertical structure and spatial scales of river plumes [Nash et al., 2009; Horner-Devine et al., 2015]. In situ measurements and satellite observation ~~performed in~~of the Yenisei and Khatanga plumes described above revealed that spatial scales of these plumes were similar, while discharge rates of the Yenisei and Khatanga rivers differed by one order of magnitude. The Yenisei and Khatanga gulfs are closely located and have similar sizes, geomorphology, and climatic conditions, albeit significantly different tidal forcing. Wind conditions several weeks before and during the field sampling were moderate and low (Fig. ~~2~~3-4), so the Yenisei and Khatanga plumes were only weakly affected by wind forcing during these periods. General shelf circulation also does not significantly impact buoyancy-driven and wind-driven spreading of the large Yenisei and Khatanga plumes [Guay et al., 2001; Panteleev et al., 2007; Zatsepin et al., 2010; 2015; Osadchiev et al., 2017; 2019]. Thus, we presume that similarity in spatial extents ~~scales~~ of these plumes is caused by difference in estuarine tidal mixing forcing that determined difference in their structure, in particular, different freshwater fractions.

The estuarine dynamical and mixing regime determined by the buoyancy and tidal forcing can be characterized by two dimensionless parameters, namely, the freshwater Froude number $Fr_f = \frac{U_R}{\sqrt{\beta g S H}}$ and a mixing parameter $M = \frac{C_D U_T^2}{w N_0 H^2}$, where U_R is the inflowing river velocity, U_T is the amplitude of the depth-averaged estuarine tidal velocity, w is the estuarine tidal frequency, S is the ambient sea salinity, H is the depth of an estuary, g is the gravity acceleration, β is the constant parameter equal to $7.7 \cdot 10^{-4}$, C_D is the constant parameter equal to 10^{-3}, $N_0 = \sqrt{\frac{\beta g S}{H}}$ is the buoyancy frequency for maximum top-to-bottom salinity variation in an estuary [Geyer and MacCready, 2014]. Values of these parameters for the Yenisei and Khatanga gulfs are the following: $Fr_f^Y \sim 0.5 / (7.7 \cdot 10^{-4} \cdot 10 \cdot 32 \cdot 10)^{0.5} \sim 0.3$, $M^Y \sim 10^{-3} \cdot (0.3)^2 / (2.3 \cdot 10^{-5} \cdot (7.7 \cdot 10^{-4} \cdot 10 \cdot 32 / 10)^{0.5} \cdot (10)^2) \sim 0.2$; $Fr_f^K \sim 0.1 / (7.7 \cdot 10^{-4} \cdot 10 \cdot 32 \cdot 10)^{0.5} \sim 0.06$, $M^K \sim 10^{-3} \cdot (0.8)^2 / (2.3 \cdot 10^{-5} \cdot (7.7 \cdot 10^{-4} \cdot 10 \cdot 32 / 10)^{0.5} \cdot (10)^2) \sim 1.8$, where the superscripts Y and K refer to the Yenisei and Khatanga gulfs, respectively. Therefore, according to classification of estuaries developed by Geyer and MacCready [2014], the Yenisei Gulf is a salt wedge estuary, while the Khatanga Gulf is characterized by strained-induced periodic stratification.

~~Freshwater fraction of a plume governs its spatial scales in a coastal sea, i.e., the same volume of freshwater can form a small freshened plume with large freshwater fraction (Fig. 6a) or a large diluted plume with small freshwater fraction (Fig. 6b). Thus, rivers with similar discharge rates can form plumes with significantly different areas. This result is in a good agreement with Fischer [1972] and Nash [2009], that showed that vertical structure and stratification of a buoyant plume is governed by both river discharge and tidal velocities. On the other hand, plumes with similar areas can be formed by rivers with significantly different discharge rates. The latter situation is the case of the Yenisei and Khatanga plumes (Fig. 5).~~

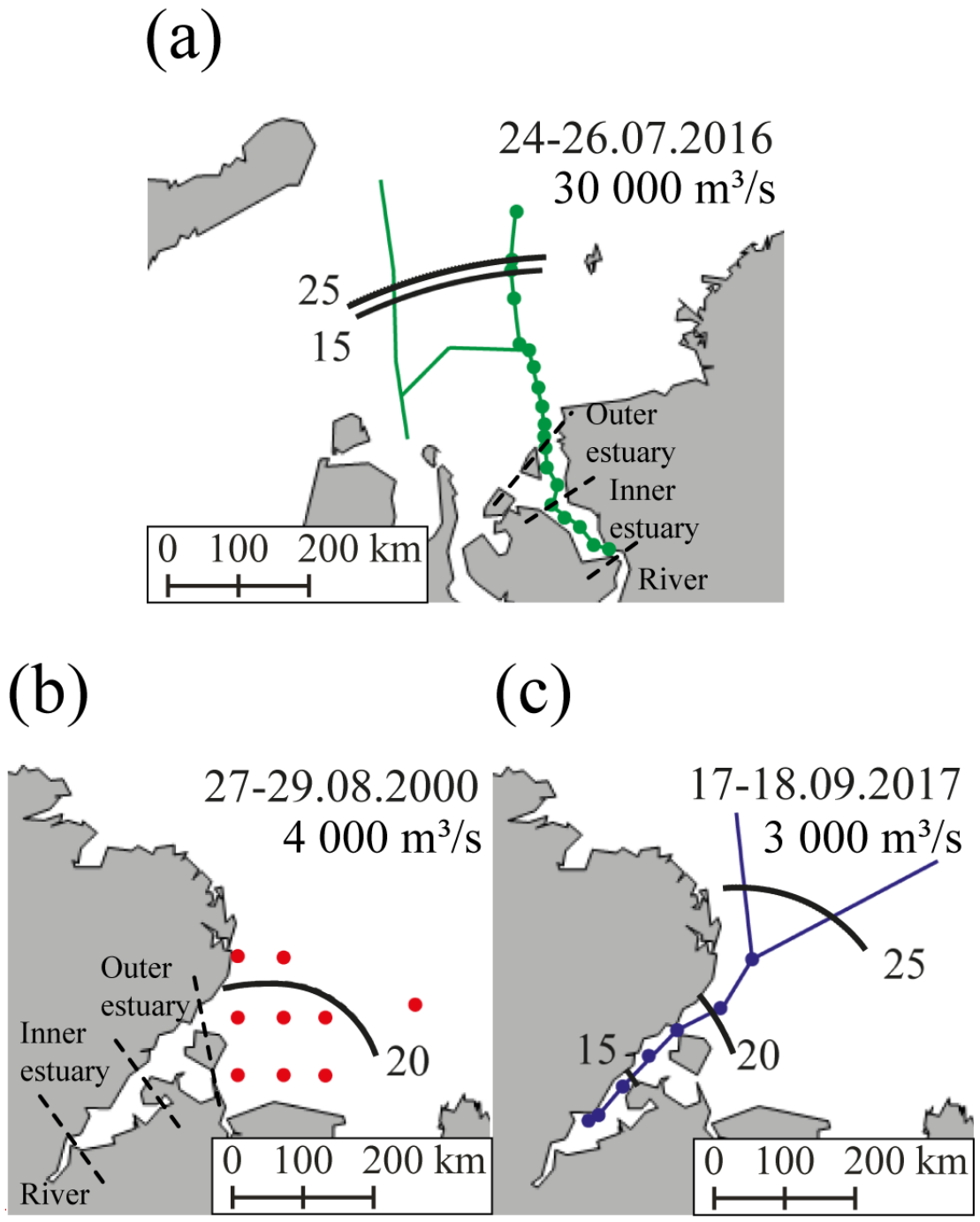

~~Figure 5: Location of isohalines of 15, 20, and 25 (black lines) at the central part of the Kara Sea (a) and the western part of the Laptev Sea (b, c) indicating spatial scales of the Yenisei (a) and Khatanga (b, c) river plumes reconstructed from in situ measurements conducted in August 2000 (red) and September 2017 (blue) in the Laptev Sea and in July 2016 (green) in the Kara Sea.~~

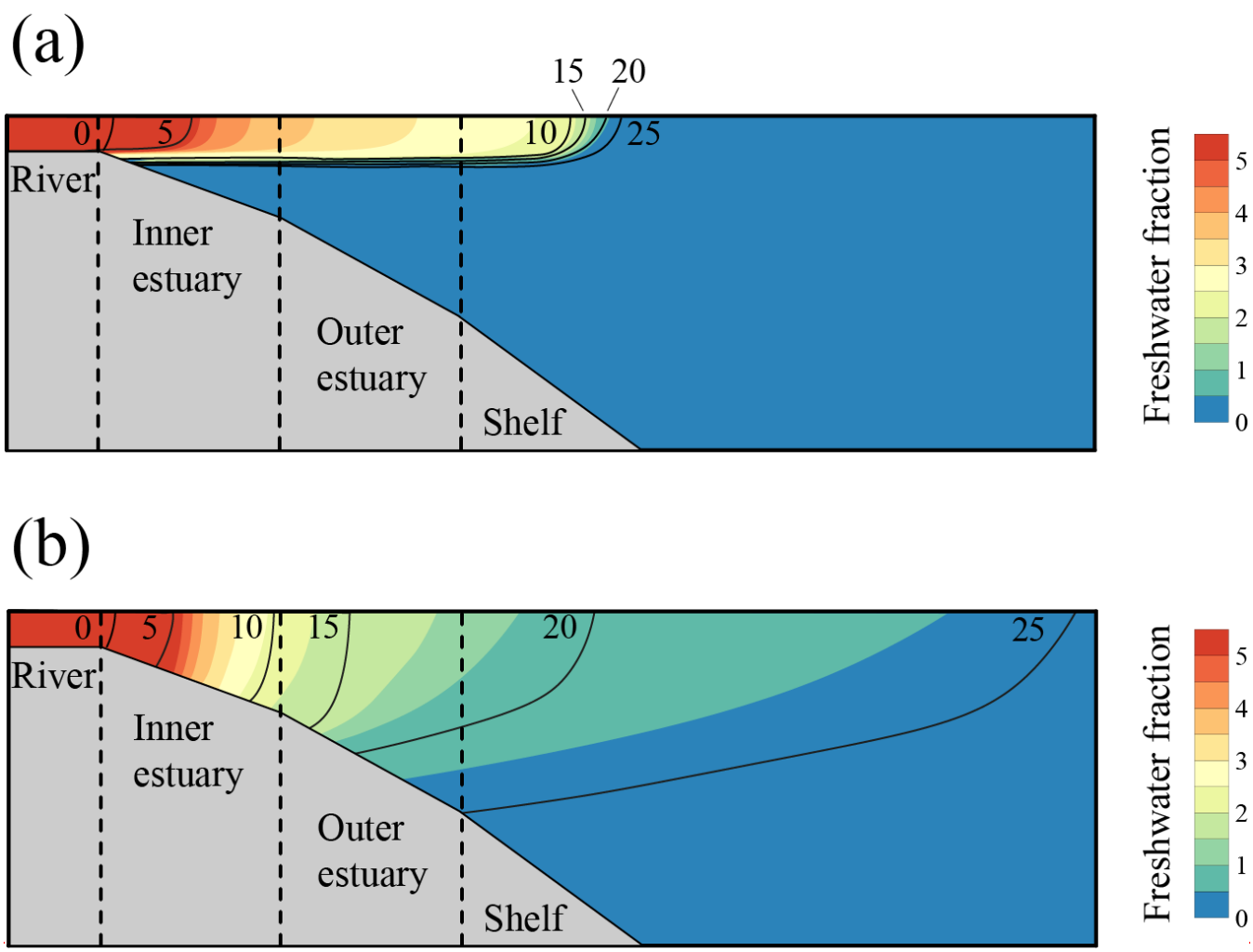

Figure 6: Schematics of vertical distribution of freshwater fraction for river plumes formed by the same volume of freshwater discharge in estuaries with low (a) and high (b) mixing forcing.

The vertical in situ measurements performed along the transects in combination with continuous salinity measurements in the surface layer along the ship track detected location of the northern plume borders defined by the isohaline of 25 (Fig. 5a, 5c). On the other hand, eastern and western segments of the plume borders and, therefore, the zonal extents of the plumes were not directly detected by in situ measurements. Nevertheless, the obtained data are representative of the total surface areas of the Yenisei and Khatanga plumes due to the following reasons. Unlike small and medium size river plumes, in which alongshore and cross shore extents can be significantly different [Yankovsky and Chapman, 1997; Fong and Geyer, 2002; Chant, 2011; Korotenko et al., 2014; Osadchiev and Sedakov, 2019], plumes formed by large rivers generally have similar zonal and meridional extents, e.g., the Amazon plume [Lentz and Limeburner, 1995; Geyer et al., 1996], the Congo plume [Denamiel et al., 2013], the Yangtze plume [Yuan et al., 2016], the Orinoco plume [Del Castillo et al., 1999], the Mississippi plume [Schiller et al., 2011]. This is also the case of the large Yenisei and Khatanga plumes formed in the semi-

~~isolated central part of the Kara Sea and western part of the Laptev Sea [Pavlov et al., 1996; Zatsepin et al., 2010; Zavialov et al., 2015]. As a result, the transects that cross the plumes from their sources in the estuaries through central parts of the plumes to their offshore parts are sufficient to quantify similarity of areas of the Yenisei and Khatanga plumes.~~

Large freshwater discharge of the Yenisei River estimated as 30000 m^3/s did not ~~exhibit~~ experience intense mixing in the estuary and formed a relatively shallow (8-12 m), low-salinity, strongly~~-~~ stratified plume (Fig. ~~3a~~5a). In situ and satellite measurements ~~along the ship track~~ showed that ~~northern~~ the boundary of the Yenisei plume was located 200-250 km from the Yenisei Gulf (Fig. ~~5a~~7a, 8). On the other hand, moderate discharge of the Khatanga River estimated as 3000 m^3/s formed anomalously deep (15-25 m), but diluted and weakly stratified plume in the middle of September 2017 (Fig. ~~4a~~6a). In situ measurements along the ship track showed that surface salinity in the southwestern part of the Laptev Sea ~~estimating~~ remained less than 25 at a distance of 200-250 km from the Khatanga Gulf (Fig. ~~5c~~7c). Another field survey conducted at the southwestern part of the Laptev Sea in the end of August 2000 (Fig. 7b), as well as satellite observations of the Khatanga plume in 2000-2019 (Fig. 9, 10) ~~also~~ confirmed ~~showed that the Khatanga plume occupied a large area (Fig. 5b). Distinct location of plume boundaries was not detected during this field survey due to absence of continuous measurements of surface salinity along the ship track. However, vertical profiles of salinity obtained at hydrological stations showed that isohaline of 20 in the surface layer was located 50-200 km from the Khatanga Gulf. It indicates~~ that spatial extents and area of the Khatanga plume formed by moderate discharge ~~(approximately 4000 m^3/s in August 2000 and 3000 m^3/s in September 2017)~~ of the Khatanga River was of the same order as the area of the Yenisei plume ~~in July 2016~~ formed by large ~~large~~ discharge ~~(approximately 30000 m^3/s)~~ of the Yenisei River.

This result is supported by vertical distributions of freshwater volume among salinity ~~layers~~ ranges in the Yenisei (Fig. ~~3c~~5c) and Khatanga (Fig. ~~4c~~6c) plumes. The majority of freshwater volume contained in the Yenisei plume in the inner estuary was located in 0-5 salinity ~~layer~~range. After the plume propagated to the outer estuary, this freshwater volume transferred to 5-10 salinity range ~~layer~~ and ~~stably~~ remained ~~in this layer~~there, when the plume was spreading over the open sea. As a result, 95% of freshwater discharge of the Yenisei River was mixed with a relatively small volume of saline sea water and formed 0-5 and 5-10 salinity ranges ~~layers~~ within the Yenisei plume with relatively small volumes. On the other hand, freshwater volume contained in the Khatanga plume steadily transferred from 0-5 salinity range ~~layer~~ near the river mouth to 20-25 salinity range ~~layer~~ in the outer estuary and sea shelf. ~~Thus~~Therefore, freshwater discharge of the Khatanga River was diluted by a large volume of saline sea water in the estuary and formed the 20-25 saline Khatanga plume with relatively large volume. This plume ~~was~~ spread~~ing~~ outside the estuary and covered wide area in the southwestern part of the Laptev Sea. ~~Thus~~Therefore, intense estuarine tidal mixing caused formation of an anomalously deep and large Khatanga plume from relatively small discharge of the Khatanga River.

In order to quantify and compare volumes of saline sea water that mix with freshwater discharge in the Yenisei and Khatanga gulfs, we used the Knudsen relations $Q_{in} = S_{out} \cdot Q_{river} / (S_{in} - S_{out})$, $Q_{out} = S_{in} \cdot Q_{river} / (S_{in} - S_{out})$, where Q_{in} and Q_{out} are the time-averaged volume fluxes from the ocean to the estuary (inflow in the bottom layer) and from the estuary to the ocean (outflow in the surface layer), S_{in} and S_{out} are the related inflow and outflow salinities, Q_{river} is the time-averaged

discharge from the river to the estuary [Knudsen, 1900; Burchard et al., 2018]. The locations of the seaward borders of the estuaries were selected at station 5336 at the Yenisei transect and station 5632 at the Khatanga transect. The inflow and outflow volume fluxes for the Yenisei Gulf during the period of in situ measurements in July 2016 are equal to $Q_{in}^{Y} \sim 8 \cdot 30000 / (32 - 8) = 10000$ m^3/s, $Q_{out}^{Y} \sim 32 \cdot 30000 / (32 - 8) = 40000$ m^3/s, while the related values for the Khatanga Gulf in September 2017 are equal to $Q_{in}^{K} \sim 22 \cdot 3000 / (32 - 22) = 6600$ m^3/s, $Q_{out}^{K} \sim 32 \cdot 3000 / (32 - 22) \sim 9600$ m^3/s. Therefore, according to this assessment, the discharge of the Khatanga River (3000 m^3/s) is mixed with twice greater volume of saline water (6600 m^3/s) in the estuary, while the discharge of the Yenisei River (30000 m^3/s) is mixed with three times less volume of saline water (10000 m^3/s) in the estuary.

According to MacCready et al. [2018], we quantified the volume-integrated net mixing N in the Yenisei and Khatanga gulfs using the relation $N = S_{in} \cdot S_{out} \cdot Q_{river}$. We obtain $N^Y \sim 32 \cdot 8 \cdot 30000 \sim 7.7 \cdot 10^6$ (g/kg)^2 m^3/s, $N^K \sim 32 \cdot 22 \cdot 3000 \sim 2.1 \cdot 10^6$ (g/kg)^2 m^3/s, that shows that tidally averaged net mixing in the Yenisei Gulf is several times greater than that in the Khatanga Gulf due to significantly greater freshwater discharge to the Yenisei Gulf, as compared to the Khatanga Gulf. This difference is even more pronounced for the inner parts of these estuaries, which borders were selected at station 5341 in the Yenisei Gulf and station 5629 in the Khatanga Gulf. The obtained values of tidally averaged net mixing in the inner estuaries were equal to $N_{inner}^{Y} \sim 25 \cdot 5 \cdot 30000 \sim 3.7 \cdot 10^6$ (g/kg)^2 m^3/s and $N_{inner}^{K} \sim 15 \cdot 11 \cdot 3000 \sim 0.5 \cdot 10^6$ (g/kg)^2 m^3/s.

The long-term average mixing values N^Y and N^K were estimated for the Yenisei and Khatanga gulfs which seaward borders were determined according to the morphology of the estuaries, i.e., based on geographical considerations. According to Burchard [2020], the same net mixing value occurs within the "estuaries" which outer borders were determined by isohalines of certain salinity $S_E = \sqrt{S_{in} S_{out}}$. This approach considers the estuarine mixing in terms of isohaline space rather than in Eulerian space and, therefore, reproduces the estuarine – river plume continuum. In particular, the values of these "estuarine salinity borders" are ~ 16 for the Yenisei plume and ~ 26.5 for the Khatanga plume. These "estuarine salinity borders" extend far off the Khatanga and Yenisei gulfs to the open sea. Moreover, they generally correspond to the plume borders (determined by the salinity isohaline of 25) due to small distance between the isohalines of 16 and 25 at the central part of the Kara Sea (Fig. 5a) and between the isohalines of 25 and 26.5 at the southwestern part of the Laptev Sea (Fig. 6a). This correspondence evidences that dynamical processes that occur in the estuaries which have relatively small areas (~10000 km^2) strongly influence spreading and mixing of the freshened surface layers over wide areas in the open sea.

~~Based on the reconstructed vertical distributions of freshwater fraction along the transects in the Yenisei and Khatanga plumes, for both transects we calculated the related transect freshwater "volumes" $T = \int_0^L (\int_{-h(x)}^0 F(x,z)dz)dx$, where x and z are the horizontal (along a transect) and vertical coordinates, respectively, $F(x, z)$ is the freshwater fraction at the point (x, z), $h(x)$ is the sea depth, L is the length of the transect. The resulting transect freshwater "volumes" of the Yenisei and Khatanga plumes, namely, T_Y and T_K, are two-dimensional. i.e., they do not consider lateral dimensions of the river plumes. However, their ratio is indicative of ratio of freshwater volumes, which are contained within these river plumes, due to similar form~~

~~and sizes of the Yenisei and Khatanga gulfs. Actually, T_Y / T_K = 46 / 5 = 9.3 that is close to ratio between discharge rates of the Yenisei and Khatanga rivers during the periods of field measurements Q_Y / Q_K = 30000 / 3000 = 10. This good agreement proves that the reconstructed distributions of freshwater fraction along the transects indeed represent distributions of volumes of freshwater discharge of the Yenisei and Khatanga rivers that formed the river plumes after being mixed with saline sea water.~~

5 Conclusions

In this study we address the Yenisei and Khatanga plumes formed by discharges of the large estuarine rivers to the Kara and Laptev seas. Based on tidal level and velocity data, tidal modelling, in situ measurements, and satellite observations, we demonstrate that estuarine tidal mixing conditions strongly affect vertical structure and spatial extents of the Yenisei and Khatanga plumes. Tidal gauge measurements and tidal modelling showed that tidal forcing is extremely intense in the Khatanga Gulf, maximal tidal velocity increases from 20–50 cm/s in the outer part of the estuary to 80–100 cm/s in its inner part. It results in intense surface-to-bottom tidal-induced mixing within the majority of the area of the Khatanga Gulf. Tidal forcing in the Yenisei Gulf, on the opposite, is relatively low (maximal tidal velocity < 25 cm/s) and limitedly affects estuarine mixing in the surface layer.

In situ salinity measurements revealed significant difference in vertical salinity structure within the Yenisei and Khatanga gulfs that induced different spreading patterns of the Yenisei and Khatanga plumes in the open sea. Freshwater discharge from the Yenisei River experienced low mixing within the Yenisei Gulf due to low-intense tidal circulation and large river runoff volume. It resulted in strong stratification between the freshened surface layer and the subjacent saline sea within the gulf. Therefore, large volume of freshwater discharge mixed with relatively small volume of saline sea water formed the Yenisei plume that propagated off the estuary and was spreading in the open sea. The low-salinity and strongly stratified Yenisei plume had relatively small depth (< 12 m), its lateral border manifested by sharp salinity gradient was located at a distance of 200-250 km from the Yenisei Gulf and 450-500 km from the Yenisei River mouth.

Freshwater discharge from the Khatanga River, on the opposite, experienced extremely strong tidal mixing in the Khatanga Gulf. Surface salinity dramatically increased within the gulf from 0 near the river mouth to 20 at the estuary mouth. However, surface salinity in the outer part of the Khatanga Gulf remained much smaller than salinity of water that inflow from the open sea to the gulf in the bottom layer, i.e., river runoff volume was large enough not to be totally mixed within the estuary and to form a freshened surface layer, albeit very diluted. As a result, the Khatanga plume that propagated off the estuary to the open sea had low freshwater fraction, i.e., it was formed by relatively small volume of freshwater discharge mixed with large volume of saline water. The low stratified Khatanga plume was very deep (up to 25 m) and occupied anomalously large area and volume (in relation to the river runoff rate) at the Laptev Sea. In situ measurements and satellite observations showed that lateral border of the Khatanga plume was located at a distance of 150-250 km from the Khatanga Gulf and 400-500 km from the Khatanga River mouth.

A number of previous works stated that river discharge rate and wind forcing are the main external conditions that govern size of a river plume [Whitney and Garvine, 2005; O'Donnell et al., 2008; Chant, 2011; Osadchiev and Zavialov, 2013; Horner-Devine et al., 2015]. In this study we show that influence of estuarine mixing on spatial scales of a large river plume in a coastal sea can be of the same importance as the roles of river discharge rate and wind forcing. The Yenisei and Khatanga plumes addressed in this work evidence that plumes with similar areas can be formed by rivers with significantly different discharge rates. Analogously, we presume that rivers with similar discharge rates can form plumes with significantly different areas in case of large differences in intensity estuarine mixing, however, the detailed analysis of this assumption is beyond the current study.

~~A number of previous works stated that river discharge rate and wind forcing are the main external conditions that govern size of a river plume [Whitney and Garvine, 2005; O'Donnell et al., 2008; Chant, 2011; Osadchiev and Zavialov, 2013; Horner-Devine et al., 2015]. In this study we show that influence of estuarine mixing on spatial scales of a large river plume in a coastal sea can be of the same importance as the roles of river discharge rate and wind forcing.~~ The ~~obtained~~ results obtained in this study allow ~~getting~~ new insights into the processes of spreading and transformation of river discharge in coastal sea. This issue is especially important for the Arctic Ocean that receives more than three-quarters of total freshwater runoff from ten large rivers [Gordeev et al., 1996; Carmack, 2000; Guay et al., 2001]. Moreover, during freshet periods in June – July the majority of annual freshwater discharge of large Arctic rivers flows into coastal areas which are mostly covered by ice. As a result, formation and spreading of these large river plumes is only weakly affected by wind forcing during these periods. ~~Thus~~Therefore, study of estuarine and deltaic mixing conditions that determine spatial scales and structure of large Arctic river plumes is essential for assessment of large-scale freshwater transport in the Arctic Ocean which plays a key role in stratification and ice formation, as well as in many physical, ~~biochemical~~biological, and ~~geological~~ geochemical processes [Carmack et al., 2010; Nummelin et al., 2016].

Data availability

Tidal gauge data were downloaded from the Unified State System of Information about the ESIMO web repository http://portal.esimo.ru/portal (available after registration). The AOTIM5 tidal model was downloaded from the Earth & Space Research (ESR) web repository https://www.esr.org/research/polar-tide-models/list-of-polar-tide-models/aotim-5/. The ERA5 atmospheric reanalysis data were downloaded from the ECMWF web repository https://www.ecmwf.int/en/forecasts/datasets/archive-datasets/reanalysis-datasets/era5. The river discharge data were downloaded from the FSHEMR web repository http://gis.vodinfo.ru/ (available after registration). The Terra/Aqua MODIS satellite data were downloaded from the NASA web repository https://ladsweb.modaps.eosdis.nasa.gov/. The in situ data are available in supplementary information.

Competing interests

The authors declare that they have no conflict of interest.

Acknowledgments

This research was funded by the Ministry of Science and Education of Russia, theme 0149-2019-0003 (collecting of in situ data); the Russian Foundation for Basic Research, research projects 18-05-60302 (processing of in situ data), 18-05-60069 (analysis of atmospheric ~~reanalysis~~ reanalysis -data), 20-35-70039 (analysis of in situ data), 18-05-60250 (tidal analysis and modelling), and 18-05-00019 (study of river plumes); the Russian Science Foundation, research project 18-17-00089 (collecting of river discharge data); the Grant of the President of the Russian Federation for state support of young Russian scientists – candidates of science, research project MK-98.2020.5 (study of freshwater transport). The river discharge data were downloaded from the repository of the Federal Service for Hydrometeorology and Environmental Monitoring of Russia http://gis.vodinfo.ru/ (available after registration). The ERA5 reanalysis data were downloaded from the European Centre for Medium-Range Weather Forecasts (ECMWF) website https://www.ecmwf.int/en/forecasts/datasets/archive-datasets/reanalysis-datasets/era5.

References

Burchard, H.: A universal law of estuarine mixing, J. Phys. Oceanogr., 50, 81-93, doi:10.1175/JPO-D-19-0014.1, 2020.

Burchard, H., Bolding, K., Feistel, R., Gräwe, U., Klingbeil, K., MacCready, P., Mohrholz, V., Umlauf, L., and van der Lee, E. M.: The Knudsen theorem and the Total Exchange Flow analysis framework applied to the Baltic Sea, Progr. Oceanogr., 165, 268–286, doi:10.1016/j.pocean.2018.04.004, 2018.

Carmack, E. C.: The freshwater budget of the Arctic Ocean: Sources, storage and sinks. In: The freshwater budget of the Arctic Ocean. E.L. Lewis, E.P. Jones (Eds.), Kluwer, Dordrecht, Netherlands, pp. 91–126, 2000.

Carmack, E. C., Yamamoto–Kawai, M., Haine, T. W., Bacon, S., Bluhm, B. A., Lique, C., Melling, H., Polyakov, I. V., Straneo, F., Timmermans, M.-L., and Williams, W. J.: Freshwater and its role in the Arctic Marine System: Sources, disposition, storage, export, and physical and biogeochemical consequences in the Arctic and global oceans, J. Geophys. Res. Biogeosciences, 121, 675–717, doi:10.1002/2015JG003140, 2016.

Chant, R. J.: Interactions between estuaries and coasts: river plumes—their formation transport and dispersal. In: Treatise on Estuarine and Coastal Science. Vol. 2. E. Wolanski, D. McLusky (Eds.), Elsevier, Amsterdam, Netherlands, pp. 213–235, 2011.

Chen, C., Guoping, G., Jianhua, Q., Proshutinsky, A., Bearsdley, R. C., Kowalik, Z., Huichan, L., and Cowles, G.: A new high-resolution unstructured grid finite volume Arctic Ocean model (AO-FVCOM): an application for tidal studies. J. Geophys. Res., 114, C08017, doi:10.1029/2008JC004941, 2009.

Dagg, M., Benner, R., Lohrenz, S., and Lawrence, D.: Transformation of dissolved and particulate materials on continental shelves influenced by large rivers: plume processes, Cont. Shelf Res., 24, 833–858, doi:10.1016/j.csr.2004.02.003, 2004.

Egbert, G. D., Bennett, A. F., and Foreman, M. G.: TOPEX/POSEIDON tides estimated using a global inverse model, J. Geophys. Res. Oceans, 99, C12, 24821–24852, doi:10.1029/94JC01894, 1994.

Fedorova, I., Chetverova, A., Bolshiyanov, D., Makarov, A., Boike, J., Heim, B., Morgenstern, A., Overduin, P.P., Wegner, C., Kashina, V., Eulenburg, V., Dobrotina, E., and Sidorina, I.: Lena Delta hydrology and geochemistry: long-term hydrological data and recent field observations, Biogeosci., 12, 345–363, doi:10.5194/bg-12-345-2015, 2015.

Fofonova, V., Danilov, S., Androsov, A., Janout, M., Bauer, M., Overduin, P., Itkin, P., and Wiltshire, K.H.: Impact of wind and tides on the Lena River freshwater plume dynamics in the summer sea, Ocean Dyn., 65, 951–968, doi: 10.1007/s10236-015-0847-573, 2015.

Garrett, C. J. R., Keeley, J. R., and Greenberg, D. A.: Tidal mixing versus thermal stratification in the Bay of Fundy and Gulf of Maine, Atmos. Ocean, 16, 403–423, doi:10.1080/07055900.1978.9649046, 1978.

Geyer, W. R., Hill, P. S., and Kineke, G. C.: The transport, transformation and dispersal of sediment by buoyant coastal flows, Cont. Shelf Res., 24, 927–949, doi:10.1016/j.csr.2004.02.006, 2004.

Geyer, W. R. and MacCready, P.: The estuarine circulation, Annu. Rev. Fluid Mech., 46, 175–197, doi:10.1146/annurev-fluid-010313-141302, 2014.

Gordeev, V. V., Martin, J. M., Sidorov, J. S., and Sidorova, M. V.: A reassessment of the Eurasian river input of water, sediment, major elements, and nutrients to the Arctic Ocean, Am. J. Sci., 296, 664–691, doi:10.2475/ajs.296.6.664, 1996.

Guay, C. K., Falkner, K. K., Muench, R. D., Mensch, M., Frank, M., and Bayer, R.: Wind-driven transport pathways for Eurasian Arctic river discharge, J. Geophys. Res., 106, C6, 11469–11480, doi:10.1029/2000JC000261, 2001.

Guo, X. and Valle-Levinson, A.: Tidal effects on estuarine circulation and outflow plume in the Chesapeake Bay, Cont. Shelf Res., 27, 20–42, doi:10.1016/j.csr.2006.08.009, 2007.

Halverson, M. J. and Palowicz, R.: Estuarine forcing of a river plume by river flow and tides, J. Geophys. Res., 113, C09033, doi:10.1029/2008JC004844, 2008.

Hetland, R. D. and Hsu, T.-J.: Freshwater and sediment dispersal in large river plumes. In: Biogeochemical Dynamics at Large River-Coastal Interfaces: Linkages with Global Climate Change. T. S. Bianchi, M. A. Allison, W.-J. Cai (Eds.), Springer, New York, USA, pp. 55–85, 2013.

Hickey, B. M., Kudela, R. M., Nash, J. D., Bruland, K. W., Peterson, W. T., MacCready, P., Lessard, E. J., Jay, D. A., Banas, N. S., Baptista, A. M., Dever, E. P., Kosro, P. M., Kilcher, L. K., Horner-Devine, A. R., Zaron, E. D., McCabe, R. M., Peterson, J. O., Orton, P. M., Pan, J., and Lohan, M. C.: River influences on shelf ecosystems: introduction and synthesis. J. Geophys. Res., 115, C00B17, doi: 10.1029/2009JC005452, 2010.

Horner-Devine, A. R., Hetland, R. D., and MacDonald, D. G.: Mixing and transport in coastal river plumes, Annu. Rev. Fluid Mech., 47, 569–594, doi:10.1146/annurev-fluid-010313-141408, 2015.

Jakobsson, M., Mayer, L., Coakley, B., Dowdeswell, J. A., Forbes, S., Fridman, B., Hodnesdal, H., Noormets, R., Pedersen, R., Rebesco, M., Schenke, H. W., Zarayskaya, Y., Accettella, D., Armstrong, A., Anderson, R. M., Bienhoff, P., Camerlenghi, A., Church, I., Edwards, M., Gardner, J. V., Hall, J. K., Hell, B., Hestvik, O., Kristoffersen, Y., Marcussen, C., Mohammad, R., Mosher, D., Nghiem, S. V., Pedrosa, M. T., Travaglini, P. G., Weatherall, P.: The international bathymetric chart of the Arctic Ocean (IBCAO) version 3.0, Geophys. Res. Lett., 39, L12609, doi:10.1029/2012GL052219 , 2012.

Johnson, D. R., McClimans, T. A., King, S., and Grenness, O.: Fresh water masses in the Kara Sea during summer, J. Mar. Sys., 12, 127–145, doi:10.1016/S0924-7963(96)00093-0, 1997.

Kagan, B. A., Timofeev, A. A., and Sofina, E. V.: Seasonal variability of surface and internal M2 tides in the Arctic Ocean, Izv. Atmos. Ocean. Phys., 46, 652–662, doi:10.1134/S0001433810050105, 2010.

Kagan, B. A., Sofina, E. V., and Timofeev, A. A.: Modeling of the M2 surface and internal tides and their seasonal variability in the Arctic Ocean: Dynamics, energetics and tidally induced diapycnal diffusion, J. Mar. Res., 69, 245–276, doi:10.1357/002224011798765312, 2011.

Knudsen, M.: Ein hydrographischer Lehrsatz, Hydrogr. Mar. Meteorol., 28, 316–320, 1900. [in German]

Korotenko, K. A., Osadchiev, A. A., Zavialov, P. O., Kao, R.-C., and Ding, C.-F.: Effects of bottom topography on dynamics of river discharges in tidal regions: case study of twin plumes in Taiwan Strait, Ocean Sci., 10, 865–879, doi: 10.5194/os-10-863-2014, 2014.

Korovkin, I. P. and Antonov, V. S.: Tides in the Khatanga River and the Khatanga Bay. Proceedings of the All-Union Scientific Research Institute, 105, 125–141, 1938. [in Russian]

Kowalik, Z. and Proshutinsky, A. Y.: The Arctic Ocean tides. In: The polar oceans and their role in shaping the global environment. Vol. 85. O. M. Johannessen, R. D. Muench, J. E. Overland (Eds.), Wiley, Washington, USA, pp. 137–158, doi:10.1029/GM085p0137, 1994.

Kulikov, M. E., Medvedev, I. P., and Kondrin, A. T.: Seasonal variability of tides in the Arctic seas, Russ. J. Earth Sci., 18, ES5003, doi:10.2205/2018ES000633, 2018.

Kulikov, M. E., Medvedev, I. P., and Kondrin, A. T.: Features of seasonal variability of tidal level oscillations in the Russian Arctic seas, Russ. Met. Hydrol., 45, 6, 2020.

Lai, Z., Ma, R., Huang, M., Chen, C., Chen, Y., Xie, C., and Beardsley, R. C.: Downwelling wind, tides, and estuarine plume dynamics, J. Geophys. Res. Oceans, 121, 4245–4263, doi:10.1002/2015JC011475, 2016.

Lebreton, L.C., Zwet, J., Damsteeg, J. W., Slat, B., Andrady, A., Reisser, J.: River plastic emissions to the world's oceans, Nat. Commun., 8, 15611, doi:10.1038/ncomms15611, 2017.

MacCready, P. and Geyer, W. R.: Advances in estuarine physics, Annu. Rev. Mar. Sci., 2, 35–58, doi:10.1146/annurev-marine-120308-081015, 2010.

MacCready, P., Geyer, W. R., and Burchard, H.: Estuarine exchange flow is related to mixing through the salinity variance budget, J. Phys. Oceanogr., 48, 1375–1384, doi:10.1175/JPO-D-17-0266.1, 2018.

Medvedev, I. P., Rabinovich, A. B., and Kulikov, E. A.: Tidal oscillations in the Baltic Sea, Oceanology, 53, 526–538, doi:10.1134/S0001437013050123, 2013.

Milliman, J. D. and Farnsworth, K. L.: River Discharge to the Coastal Ocean: A Global Synthesis. Cambridge University Press, Cambridge, UK, doi:0.1017/CBO9780511781247, 2011.

Nash, J. D., Kilcher, L. F., and Moum, J. N.: Structure and composition of a strongly stratified, tidally pulsed river plume, J. Geophys. Res., 114, C00B12, doi:10.1029/2008JC005036, 2009.

Nummelin, A., Ilicak, M., Li, C., and Smedsrud, L. H.: Consequences of future increased Arctic runoff on Arctic Ocean stratification, circulation, and sea ice cover, J. Geophys. Res. Oceans, 121, 617–637, doi:10.1002/2015JC011156, 2016.

O'Donnell, J., Ackleson, S. G., and Levine, E. R.: On the spatial scales of a river plume, J. Geophys. Res., 113, C04017, doi:10.1029/2007JC004440, 2008.

O'Reilly, J. E., Maritorena, S., Mitchell, B. G., Siegel, D. A., Carder, K. L., Garver, S. A., Kahru, M., and McClain, C. R.: Ocean color chlorophyll algorithms for SeaWiFS, J. Geophys. Res., 103, 24937–24953, doi:10.1029/98JC02160, 1998.

Osadchiev, A.A.: Spreading of the Amur river plume in the Amur Liman, the Sakhalin Gulf, and the Strait of Tartary, Oceanology, 57, 376–382, doi: 10.1134/S0001437017020151, 2017.

Osadchiev, A.A., Asadulin, En.E., Miroshnikov, A.Yu., Zavialov, I.B., Dubinina, E.O., Belyakova, P.A.: Bottom sediments reveal inter-annual variability of interaction between the Ob and Yenisei plumes in the Kara Sea, Sci. Rep., 9, 18642, doi:10.1038/s41598-019-55242-3, 2019.

Osadchiev, A. A., Izhitskiy, A. S., Zavialov, P. O., Kremenetskiy, V. V., Polukhin, A. A., Pelevin, V. V., and Toktamysova, Z. M.: Structure of the buoyant plume formed by Ob and Yenisei river discharge in the southern part of the Kara Sea during summer and autumn, J. Geophys. Res. Oceans, 122, 5916–5935, doi:10.1002/2016JC012603, 2017.

Osadchiev, A. and Korshenko, E.: Small river plumes off the northeastern coast of the Black Sea under average climatic and flooding discharge conditions, Ocean Sci., 13, 465–482, doi:10.5194/os-13-465-2017, 2017.

Osadchiev, A.A. and Sedakov, R.O.: Spreading dynamics of small river plumes off the northeastern coast of the Black Sea observed by Landsat 8 and Sentinel-2, Rem. Sens. Environ., 221, 522–533, doi:10.1016/j.rse.2018.11.043, 2019.

Osadchiev A. and Zavialov, P.: Lagrangian model of a surface-advected river plume, Cont. Shelf Res., 58, 96–106, doi: 10.1016/j.csr.2013.03.010, 2013.

Padman, L. and Erofeeva, S.: A barotropic inverse tidal model for the Arctic Ocean. Geophys. Res. Lett., 31, L02303, doi:10.1029/2003GL019003, 2004.

Panteleev, G., Proshutinsky, A., Kulakov, M., Nechaev, D. A., and Maslowski W.: Investigation of the summer Kara Sea circulation employing a variational data assimilation technique, J. Geophys. Res.,112, C04S15, doi:10.1029/2006JC003728, 2007.

Pavlov, V. K., Timokhov, L. A., Baskakov, G. A., Kulakov, M. Y., Kurazhov, V. K., Pavlov, P. V., Pivovarov, S. V., and Pawlowicz, R., Beardsley, B., and Lentz, S.: Classical tidal harmonic analysis including error estimates in MATLAB using

T_TIDE, Comput. Geosci., 28, 929–937, doi:10.1016/S0098-3004(02)00013-4, 2002.Simpson, J. H. and Hunter, J. R.: Fronts in the Irish Sea, Nature, 250, 404–406, doi:10.1038/250404a0, 1974.

Stanovoy, V. V.: Hydrometeorological regime of the Kara, Laptev, and East-Siberian seas. Technical Memorandum, APL-UW TM 1-96, Applied Physics Laboratory, University of Washington, 1996.

Schettini, C. A. F., Kuroshima, K. N., Fo, J. P., Rorig, L. R., and Resgalla Jr., C.: Oceanographic and ecological aspects of the Itajai-Acu River plume during a high discharge period, An. Acad. Bras. Ci., 70, 335–352, 1998.

Schmidt, C., Krauth, T., and Wagner, S.: Export of plastic debris by rivers into the sea, Environ. Sci. Technol., 51, 21, 12246–12253, doi:10.1021/acs.est.7b02368, 2017.

Voinov, G.: Tide and tidal streams. In: Polar Seas Oceanography: an integrated case study of the Kara Sea. V.A. Volkov, O.M. Johannessen, V.E. Borodachev, G.N. Voinov, L.H. Pettersson, L.P. Bobylev, A.V. Kouraev (Eds.), Springer, Berlin, Germany, pp. 147-216, 2002.

Werdell, P. J., and Bailey, S. W.: An improved bio-optical data set for ocean color algorithm development and satellite data product validation, Rem. Sens. Environ., 98, 122–140, doi:10.1016/j.rse.2005.07.001, 2005.

Williams, W. J. and Carmack, E. C.: The 'interior' shelves of the Arctic Ocean: Physical oceanographic setting, climatology and effects of sea-ice retreat on cross-shelf exchange, Prog. Oceanogr., 139, 24–31, doi:10.1016/j.pocean.2015.07.008, 2015.

Whitney, M. M. and Garvine, R. W.: Wind influence on a coastal buoyant outflow, J. Geophys. Res., 110, C03014, doi:10.1029/2003jc002261, 2005.

Zatsepin, A. G., Zavialov, P. O., Kremenetskiy, V. V., Poyarkov, S. G., and Soloviev, D. M.: The upper desalinated layer in the Kara Sea, Oceanology, 50, 657–667, doi:10.1134/s0001437010050036, 2010.

Zavialov, I. B., Osadchiev, A. A., Sedakov, R. O., Barnier, B., Molines, J.-M., and Belokopytov, V.N.: Water exchange between the Sea of Azov and the Black Sea through the Kerch Strait, Ocean Sci., 16, 15–30, doi:10.5194/os-16-15-2019, 2020.

Zavialov, P. O., Izhitskiy, A. S., Osadchiev, A. A., Pelevin, V. V., and Grabovskiy, A. B.: The structure of thermohaline and bio-optical fields in the upper layer of the Kara Sea in September 2011, Oceanology, 55, 461–471, doi:10.1134/s0001437015040177, 2015.~~Carmack, E. C.: The freshwater budget of the Arctic Ocean: Sources, storage and sinks. In: The freshwater budget of the Arctic Ocean. E.L. Lewis, E.P. Jones (Eds.), Kluwer, Dordrecht, Netherlands, pp. 91–126, 2000.~~

~~Carmack, E. C., Yamamoto-Kawai, M., Haine, T. W., Bacon, S., Bluhm, B. A., Lique, C., Melling, H., Polyakov, I. V., Straneo, F., Timmermans, M. L., and Williams, W. J.: Freshwater and its role in the Arctic Marine System: Sources, disposition, storage, export, and physical and biogeochemical consequences in the Arctic and global oceans, J. Geophys. Res. Biogeosciences, 121, 675–717, doi:10.1002/2015JG003140, 2016.~~

~~Chant, R. J.: Interactions between estuaries and coasts: river plumes—their formation transport and dispersal. In: Treatise on Estuarine and Coastal Science. Vol. 2. E. Wolanski, D. McLusky (Eds.), Elsevier, Amsterdam, Netherlands, pp. 213–235, 2011.~~

Dagg, M., Benner, R., Lohrenz, S., and Lawrence, D.: Transformation of dissolved and particulate materials on continental shelves influenced by large rivers: plume processes, Cont. Shelf Res., 24, 833–858, doi:10.1016/j.csr.2004.02.003, 2004.

Del Castillo, C. E., Coble, P. G., Morell, J. M., Lopez, J. M., and Corredor, J. E.: Analysis of the optical properties of the Orinoco River plume by absorption and fluorescence spectroscopy, Mar. Chem., 66, 35–51, doi:10.1016/s0304-4203(99)00023-7, 1999.

Denamiel, C., Budgell, W. P., and Toumi, R.: The Congo River plume: Impact of the forcing on the far-field and near-field dynamics, J. Geophys. Res., 118, 964–989, doi:10.1002/jgrc.20062, 2013.

Fischer, H. B.: Mass transport mechanisms in partially stratified estuaries, J. Fluid. Mech., 53, 671–687, doi:10.1017/S0022112072000412, 1972.

Fong, D. A. and Geyer, W. R.: The alongshore transport of freshwater in a surface-trapped river plume, J. Phys. Oceanogr., 32, 957–972, doi:10.1175/1520-0485(2002)032<0957:TATOFI>2.0.CO;2, 2002.

Geyer W. R., Beardsley, R. C., Lentz, S. J., Candela, J., Limeburner, R., Johns, W. E., Castro, B. M., and Soares, I. D.: Physical oceanography of the Amazon shelf, Cont. Shelf Res., 16, 575–616, doi:10.1016/0278-4343(95)00051-8, 1996.

Geyer, W. R., Hill, P. S., and Kineke, G. C.: The transport, transformation and dispersal of sediment by buoyant coastal flows, Cont. Shelf Res., 24, 927–949, doi:10.1016/j.csr.2004.02.006, 2004.

Geyer, W. R. and MacCready, P.: The estuarine circulation, Annu. Rev. Fluid Mech., 46, 175–197, doi:10.1146/annurev-fluid-010313-141302, 2014.

Gordeev, V. V., Martin, J. M., Sidorov, J. S., and Sidorova, M. V.: A reassessment of the Eurasian river input of water, sediment, major elements, and nutrients to the Arctic Ocean, Am. J. Sci., 296, 664–691, doi:10.2475/ajs.296.6.664, 1996.

Guay, C. K., Falkner, K. K., Muench, R. D., Mensch, M., Frank, M., and Bayer, R.: Wind driven transport pathways for Eurasian Arctic river discharge, J. Geophys. Res., 106, C6, 11469–11480, doi:10.1029/2000JC000261, 2001.

Guo, X. and Valle-Levinson, A.: Tidal effects on estuarine circulation and outflow plume in the Chesapeake Bay, Cont. Shelf Res., 27, 20–42, doi:10.1016/j.csr.2006.08.009, 2007.

Halverson, M. J. and Palowicz, R.: Estuarine forcing of a river plume by river flow and tides, J. Geophys. Res., 113, C09033, doi:10.1029/2008JC004844, 2008.

Hetland, R. D. and Hsu, T. J.: Freshwater and sediment dispersal in large river plumes. In: Biogeochemical Dynamics at Large River Coastal Interfaces: Linkages with Global Climate Change. T. S. Bianchi, M. A. Allison, W. J. Cai (Eds.), Springer, New York, USA, pp. 55–85, 2013.

Hickey, B. M., Kudela, R. M., Nash, J. D., Bruland, K. W., Peterson, W. T., MacCready, P., Lessard, E. J., Jay, D. A., Banas, N. S., Baptista, A. M., Dever, E. P., Kosro, P. M., Kilcher, L. K., Horner-Devine, A. R., Zaron, E. D., McCabe, R. M., Peterson, J. O., Orton, P. M., Pan, J., and Lohan, M. C.: River influences on shelf ecosystems: introduction and synthesis. J. Geophys. Res., 115, C00B17, doi: 10.1029/2009JC005452, 2010.

Horner-Devine, A. R., Hetland, R. D., and MacDonald, D. G.: Mixing and transport in coastal river plumes, Annu. Rev. Fluid Mech., 47, 569–594, doi:10.1146/annurev-fluid-010313-141408, 2015.

Johnson, D. R., McClimans, T. A., King, S., and Grenness, O.: Fresh water masses in the Kara Sea during summer, J. Mar. Sys., 12, 127–145, doi:10.1016/S0924-7963(96)00093-0, 1997.

Kagan, B. A., Timofeev, A. A., and Sofina, E. V.: Seasonal variability of surface and internal M2 tides in the Arctic Ocean, Izv. Atmos. Ocean. Phys., 46, 652–662, doi:10.1134/S0001433810050105, 2010.

Kagan, B. A., Sofina, E. V., and Timofeev, A. A.: Modeling of the M2 surface and internal tides and their seasonal variability in the Arctic Ocean: Dynamics, energetics and tidally induced diapycnal diffusion, J. Mar. Res., 69, 245–276, doi:10.1357/002224011798765312, 2011.

Korotenko, K. A., Osadchiev, A. A., Zavialov, P. O., Kao, R. C., and Ding, C. F.: Effects of bottom topography on dynamics of river discharges in tidal regions: case study of twin plumes in Taiwan Strait, Ocean Sci., 10, 865–879, doi:10.5194/os-10-863-2014, 2014.

Korovkin, I. P. and Antonov, V. S.: Tides in the Khatanga River and the Khatanga Bay. Proceedings of the All-Union Scientific Research Institute, 105, 125–141, 1938. [in Russian]

Kulikov, M. E., Medvedev, I. P., and Kondrin, A. T.: Seasonal variability of tides in the Arctic seas, Russ. J. Earth Sci., 18, ES5003, doi:10.2205/2018ES000, 2018.

Lai, Z., Ma, R., Huang, M., Chen, C., Chen, Y., Xie, C., and Beardsley, R. C.: Downwelling wind, tides, and estuarine plume dynamics, J. Geophys. Res. Oceans, 121, 4245–4263, doi:10.1002/2015JC011475, 2016.

Lebreton, L.C., Zwet, J., Damsteeg, J. W., Slat, B., Andrady, A., Reisser, J.: River plastic emissions to the world's oceans, Nat. Commun., 8, 15611, doi:10.1038/ncomms15611, 2017.

Lentz, S. J. and Limeburner, R.: The Amazon River Plume during AMASSEDS: Spatial characteristics and salinity variability, J. Geophys. Res. Oceans, 100, 2355–2375, doi:10.1029/94jc01411, 1995.

MacCready, P. and Geyer, W. R.: Advances in estuarine physics, Annu. Rev. Mar. Sci., 2, 35–58, doi:10.1146/annurev-marine-120308-081015, 2010.

Milliman, J. D. and Farnsworth, K. L.: River Discharge to the Coastal Ocean: A Global Synthesis. Cambridge University Press, Cambridge, UK, doi:0.1017/CBO9780511781247, 2011.

Nash, J. D., Kilcher, L. F., and Moum, J. N.: Structure and composition of a strongly stratified, tidally pulsed river plume, J. Geophys. Res., 114, C00B12, doi:10.1029/2008JC005036, 2009.

Nummelin, A., Ilicak, M., Li, C., and Smedsrud, L. H.: Consequences of future increased Arctic runoff on Arctic Ocean stratification, circulation, and sea ice cover, J. Geophys. Res. Oceans, 121, 617–637, doi:10.1002/2015JC011156, 2016.

O'Donnell, J., Ackleson, S. G., and Levine, E. R.: On the spatial scales of a river plume, J. Geophys. Res., 113, C04017, doi:10.1029/2007JC004440, 2008.

Osadchiev, A.A., Asadulin, En.E., Miroshnikov, A.Yu., Zavialov, I.B., Dubinina, E.O., Belyakova, P.A.: Bottom sediments reveal inter-annual variability of interaction between the Ob and Yenisei plumes in the Kara Sea, Sci. Rep., 9, 18642, doi:10.1038/s41598-019-55242-3, 2019.

Osadchiev, A. A., Izhitskiy, A. S., Zavialov, P. O., Kremenetskiy, V. V., Polukhin, A. A., Pelevin, V. V., and Toktamysova, Z. M.: Structure of the buoyant plume formed by Ob and Yenisei river discharge in the southern part of the Kara Sea during summer and autumn, J. Geophys. Res. Oceans, 122, 5916–5935, doi:10.1002/2016JC012603, 2017.

Osadchiev, A. and Korshenko, E.: Small river plumes off the northeastern coast of the Black Sea under average climatic and flooding discharge conditions, Ocean Sci., 13, 465–482, doi:10.5194/os-13-465-2017, 2017.

Osadchiev, A.A. and Sedakov, R.O.: Spreading dynamics of small river plumes off the northeastern coast of the Black Sea observed by Landsat 8 and Sentinel-2, Rem. Sens. Environ., 221, 522–533, doi:10.1016/j.rse.2018.11.043, 2019.

Osadchiev A. and Zavialov, P.: Lagrangian model of a surface-advected river plume, Cont. Shelf Res., 58, 96–106, doi:10.1016/j.csr.2013.03.010, 2013.

Padman, L. and Erofeeva, S.: A barotropic inverse tidal model for the Arctic Ocean. Geophys. Res. Lett., 31, L02303, doi:10.1029/2003GL019003, 2004.

Panteleev, G., Proshutinsky, A., Kulakov, M., Nechaev, D. A., and Maslowski W.: Investigation of the summer Kara Sea circulation employing a variational data assimilation technique, J. Geophys. Res.,112, C04S15, doi:10.1029/2006JC003728, 2007.

Pavlov, V. K., Timokhov, L. A., Baskakov, G. A., Kulakov, M. Y., Kurazhov, V. K., Pavlov, P. V., Pivovarov, S. V., and Stanovoy, V. V.: Hydrometeorological regime of the Kara, Laptev, and East Siberian seas. Technical Memorandum, APL-UW TM 1-96, Applied Physics Laboratory, University of Washington, 1996.

Schettini, C. A. F., Kuroshima, K. N., Fo, J. P., Rorig, L. R., and Resgalla Jr., C.: Oceanographic and ecological aspects of the Itajai-acu River plume during a high discharge period, An. Acad. Bras. Ci., 70, 335–352, 1998.

Schiller, R. V., Kourafalou, V. H., Hogan, P., Walker, N. D.: The dynamics of the Mississippi River plume: Impact of topography, wind and offshore forcing on the fate of plume waters, J. Geophys. Res. Oceans, 116, C6, doi:10.1029/2010jc006883, 2011.

Schmidt, C., Krauth, T., and Wagner, S.: Export of plastic debris by rivers into the sea, Environ. Sci. Technol., 51, 21, 12246–12253, doi:10.1021/acs.est.7b02368, 2017.

Williams, W. J. and Carmack, E. C.: The 'interior' shelves of the Arctic Ocean: Physical oceanographic setting, climatology and effects of sea-ice retreat on cross-shelf exchange, Prog. Oceanogr., 139, 24–31, doi:10.1016/j.pocean.2015.07.008, 2015.

Whitney, M. M. and Garvine, R. W.: Wind influence on a coastal buoyant outflow, J. Geophys. Res., 110, C03014, doi:10.1029/2003jc002261, 2005.

Yankovsky, A. E. and Chapman, D. C.: A simple theory for the fate of buoyant coastal discharges, J. Phys. Oceanogr., 27, 1386–1401, doi:10.1175/1520-0485(1997)027<1386:astftf>2.0.co;2, 1997.

Yuan, R., Wu, H., Zhu, J., and Li, L.: The response time of the Changjiang plume to river discharge in summer, J. Mar. Syst., 154, 82–92, doi:10.1016/j.jmarsys.2015.04.001, 2016.

Zatsepin, A. G., Zavialov, P. O., Kremenetskiy, V. V., Poyarkov, S. G., and Soloviev, D. M.: The upper desalinated layer in the Kara Sea, Oceanology, 50, 657–667, doi:10.1134/s0001437010050036, 2010.

Zavialov, P. O., Izhitskiy, A. S., Osadchiev, A. A., Pelevin, V. V., and Grabovskiy, A. B.: The structure of thermohaline and bio-optical fields in the upper layer of the Kara Sea in September 2011, Oceanology, 55, 461–471, doi:10.1134/s0001437015040177, 2015.